electronics

MDPI

Review

Recent Developments in Bidirectional DC-DC Converter Topologies, Control Strategies, and Applications in Photovoltaic Power Generation Systems: A Comparative Review and Analysis

Ayiguzhali Tuluhong [1,2], Zhisen Xu [1,2,*], Qingpu Chang [1,2] and Tengfei Song [1,2]

[1] College of Electrical Engineering, Xinjiang University, Urumqi 830047, China; lazugia@xju.edu.cn (A.T.); 107552304482@stu.xju.edu.cn (Q.C.); 107552301538@stu.xju.edu.cn (T.S.)
[2] The Engineering Research Center of Education Ministry for Renewable Energy Power Generation and Grid-Connected Control, Urumqi 830047, China
* Correspondence: 107552304527@stu.xju.edu.cn; Tel.: +86-13461377680

Abstract: As an important piece of equipment in photovoltaic power generation systems, the bidirectional DC-DC converter plays a vital role in improving the conversion efficiency of photovoltaic power generation system. The energy transfer in PV systems heavily relies on efficient bidirectional DC-DC converters. To ensure stable operation, converters with high reliability and power density are required. This paper introduces the basic principles and topologies of bidirectional DC-DC converters and provides a comparative analysis. And it examines the characteristics of the converters' control schemes and switching strategies, summarizes the existing research findings and current issues. Finally, it looks ahead to the future development trends of bidirectional DC-DC converters in PV systems.

Keywords: bidirectional DC-DC converter; power electronics topology; control scheme; switching strategy

Academic Editor: Nilanjan Ray Chaudhuri

Received: 29 November 2024
Revised: 5 January 2025
Accepted: 10 January 2025
Published: 20 January 2025

Citation: Tuluhong, A.; Xu, Z.; Chang, Q.; Song, T. Recent Developments in Bidirectional DC-DC Converter Topologies, Control Strategies, and Applications in Photovoltaic Power Generation Systems: A Comparative Review and Analysis. *Electronics* **2025**, *14*, 389. https://doi.org/10.3390/electronics14020389

1. Introduction

The extensive use of fossil fuels such as oil, coal, and natural gas have caused a serious greenhouse effect and environmental pollution, which has a significant impact on the environment [1]. At the same time, there is also a big contradiction between the supply capacity of fossil fuels and the total global energy demand. With the global energy shortage, the general trend is to vigorously develop renewable energy. Among the many clean energy sources [2], the development and utilization of solar energy accounts for the highest proportion, and solar energy also has the most potential for development. Photovoltaic power generation is one of the important components of the world's energy in the past few decades, because of its easy installation, low operating costs, mature technology, and other characteristics. It has become one of the most practical renewable energy technologies. The global growth of photovoltaic power generation systems (PSG) [3] is very rapid and varies greatly between countries. The International Energy Agency (IEA) estimates that the new installed capacity of renewable energy will reach 507 GW in 2023, nearly 50% higher than in 2022. Due to China's strong development of solar and wind energy, in the next five years, the capacity of newly installed renewable energy will continue to increase; solar and wind accounted for 96% of the record. Figure 1 shows the new renewable electricity capacity, by technology, from 2016 to 2028.

By 2028, the global electricity mix will be transformed, with 3700 GW of the new renewable energy capacity connected to the grid between 2023 and 2028. Renewables

account for more than 42% of global electricity generation, with wind and solar set to account for 25%. Figure 2 shows the share of renewable energy by technology for 2000–2028.

PV panels have the characteristics of low voltage and high current, which requires the converter to have a high voltage boost capacity to efficiently convert and use electrical energy. To ensure that the electric vehicle converter can quickly charge the battery, which requires high power and high current output, the control strategy is also inclined towards a constant current and constant voltage control, allowing for the car to move forward stably. The uninterruptible power supply is mainly used as a backup power supply to provide temporary power when the main power supply fails to protect critical loads from power outages. The control strategy focuses on dynamic response and multi-mode control. All converters can be used in PGS as long as they can achieve high voltage gain, high efficiency, and a wide voltage range in a low duty cycle [4].

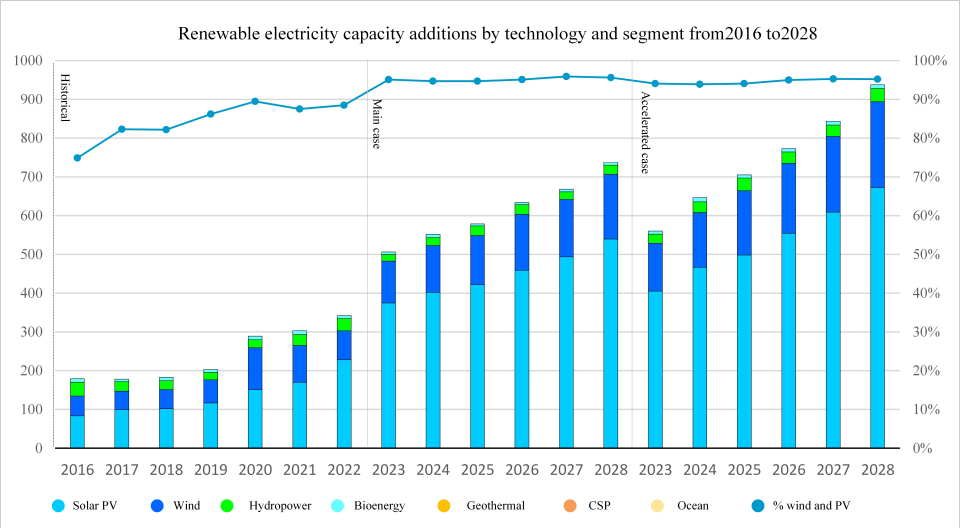

Figure 1. New renewable energy electricity capacity by technology from 2016 to 2028.

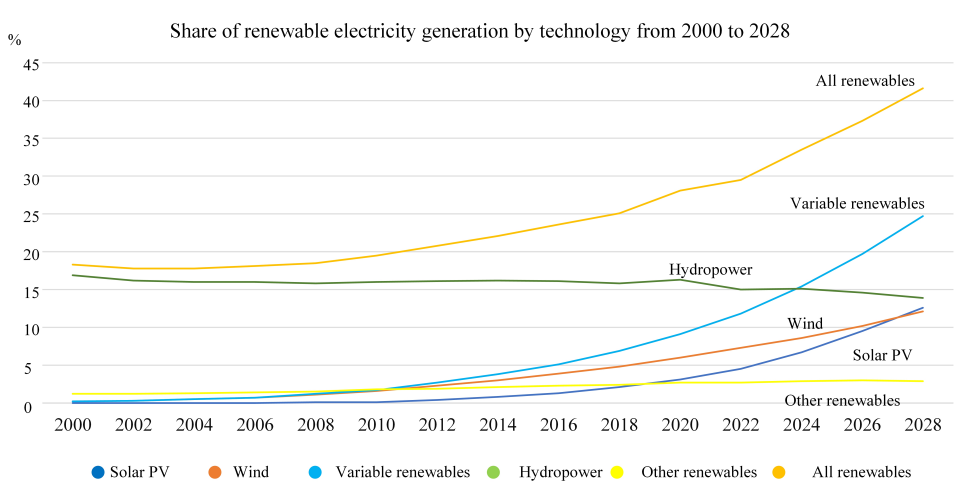

Figure 2. Renewable energy share by technology from 2000 to 2028.

The electricity generated by PGS is affected by weather and lighting conditions, and has intermittent and random volatility, resulting in the reduced reliability of the power supply and a negative impact on load. Combining the corresponding power supply with energy storage can improve this situation. The bidirectional DC converter can store excess electrical energy in the battery when the electrical energy generated by the solar panel

is greater than the load demand, and release energy from the battery to meet the load demand when the electrical energy demand is greater than the PGS supply. At the same time, the bidirectional DC converter can maintain the stability of the DC bus voltage, which is very important to ensure the reliability and stability of the system [5]. In addition, it can also adjust the working state of the PV panel through the maximum power point algorithm to ensure that it is always working at the maximum power point and improve energy conversion efficiency. The PGS can realize the efficient conversion and stable output of electric energy through the bidirectional DC-DC converter, make up for the defects of the solar PGS such as discontinuity and instability, and improve the overall system efficiency. The overall structure diagram is shown in Figure 3. DC-DC converters can be divided into non-isolated DC-DC converters [6] and isolated DC-DC converters [7] according to whether there is a transformer. Non-isolated DC-DC converters have simple structure and do not need to use transformers for electrical isolation between input and output, so they are smaller in size and lower in cost. At the same time, the non-isolated DC-DC converter does not have the process of transformer magnetoelectric conversion, and the efficiency is generally higher. For PGS, there is a difference of more than 10 times between the output voltage of the photovoltaic cell array and the input voltage required for a grid-connected or power converter. Although the traditional boost converter can realize the boost voltage, its voltage gain is limited by the duty cycle, and it is not suitable for high gain conversion. To solve this problem, scholars through the construction of circuit topology, high-gain non-isolated DC-DC converters can be divided into interleaved type, cascade type, multilevel type, with switched capacitor/inductor boost unit and coupled inductor type. It also has disadvantages, if any problem occurs at the output side, it will affect the input side. In order to overcome this shortcoming, isolated DC-DC converters can be used, which can achieve electrical isolation through transformers [8], which can provide electrical isolation [9], enhance safety, reduce electromagnetic interference [10], and effectively isolate the input and output. However, the transformer will lose some energy in the electromagnetic conversion process, resulting in the low efficiency of the converter. In addition, due to the influence of the transformer leakage, the inductor current ripple [11] will also increase, which limits its application range. Nevertheless, isolated DC-DC converters are still suitable for high-power applications where safety requirements are high or electrical isolation is required.

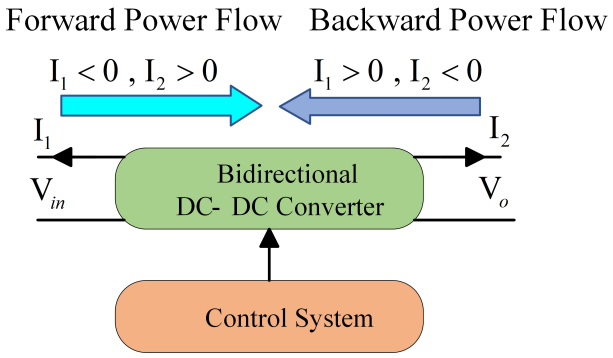

Figure 3. Overall structure diagram of bidirectional DC-DC converter.

In this paper, bidirectional DC-DC converters are classified into two types: non-isolated type and isolated type according to the isolation function. Figure 4 shows the classification of DC-DC converters. The topologies, working principles and control strategies of various converters are discussed in detail. In addition, their performance and their advantages and disadvantages are also analyzed. The rest of this article is organized as follows: Section 2 covers the classification of DC-DC converters, Section 3 covers non-isolated

topologies, and Section 4 covers isolated topologies. Section 5 introduces the three-port converter, Section 6 introduces the switching strategy, Section 7 introduces the control strategy, and Section 8 is the conclusion of this paper.

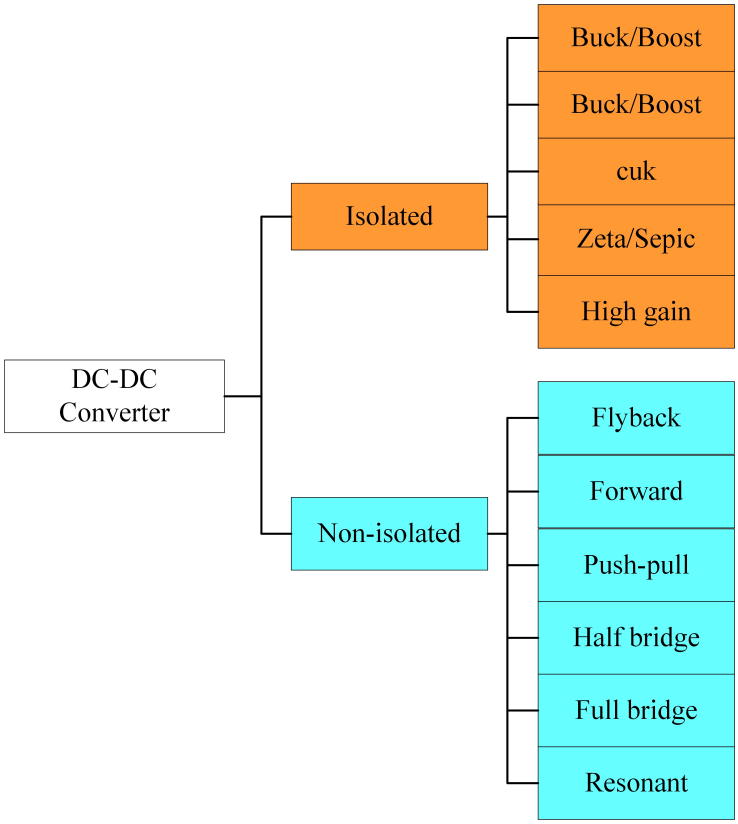

Figure 4. Classification of DC-DC converters.

2. Bidirectional DC-DC Converter Topology Classification

According to published industry research results, bidirectional DC-DC converters are classified into non-isolated and isolated types according to whether they have an isolation function. Non-isolated bidirectional DC-DC converters include bidirectional buck/boost, bidirectional buck–boost, bidirectional Cuk, bidirectional Zeta/Sepic and high-increase DC converters, while isolated types include bidirectional flyback, bidirectional forward, bidirectional push pull, bidirectional half bridge, bidirectional full bridge and DAB converter. According to the input circuit type, there is the voltage source type and the current source type; if according to the basic unit expansion, there are series type, parallel type, combined type and compound bidirectional DC-DC converters, and according to the input port classification, there are two ports and multi-ports. In terms of technology, there are soft switches and reactive switches. The classification of DC-DC converters is shown in Figure 4. In this paper, the converter will be described from two categories: the isolated type and non-isolated type.

3. Non-Isolated Bidirectional DC-DC Converter Topology

3.1. Bidirectional Buck/Boost Converter

The bidirectional buck/boost converter [12,13] is constructed based on the unidirectional buck or boost converter, meaning that the diode and the power tube are in reverse parallel at both ends of the original power tube and diode, and its topology is shown in Figure 5. The bidirectional buck/boost converter has the advantages of simple topology and control strategy, fewer required devices, and high conversion efficiency. However, due

to the inherent structure of the converter, the input and output voltage conversion ratio is relatively small, so it is only suitable for low-power applications without electrical isolation.

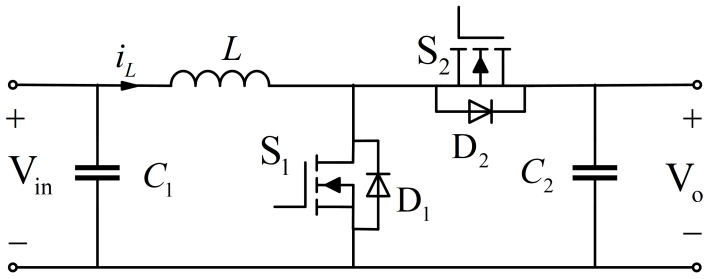

Figure 5. Topology of bidirectional buck/boost converter.

The zero-voltage switching (ZVS) condition can be achieved by the switch's parallel diode conduction. The parallel diode will conduct just before the switch's turn-on moment so that the switch's voltage will be fixed at zero and the switch will turn on with soft switching condition [14]. In order to achieve the soft switching conditions of traditional buck converters, reference [15] added LC auxiliary circuits to the switches. When the switch is turned off, the current of the capacitor is discharged through the resonant capacitor, causing the voltage across the switch to gradually decrease to zero, achieving ZVS, and the output current ripple is almost zero. The converter proposed in reference [16] uses coupled inductors and diodes to greatly improve voltage gain. By using coupled inductors and clamping circuits, the voltage stress on the main switch and diode is effectively reduced, thus allowing the use of devices with lower voltage levels and reducing on–off losses. However, during the switching process, due to the influence of parasitic capacitance and leakage induction, additional voltage stress may be generated.

3.2. Bidirectional Buck–Boost Converter

The bidirectional buck–boost converter is composed of a reverse diode on the primary power switch and a reverse power switch on the primary diode of the unidirectional buck–boost converter. Its topology is shown in Figure 6. The bidirectional buck–boost converter can realize both voltage boost and voltage drop in the same transmission direction. It has a wide range of voltage regulation, simple topology, easy design of control and drive circuits, and is suitable for low-power applications. When $V_1 > V_2$, power transfers from the power supply to the battery in charging mode (buck mode); when $V_1 < V_2$, power transfers from the battery to the power supply during discharge mode (boost mode). When $D < 0.5$, the operation is in step-down mode; when $D > 0.5$, it works in boost mode.

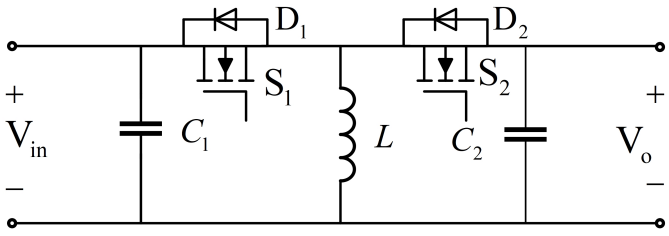

Figure 6. Topology of bidirectional buck–boost converter.

Reference [17] introduces a new zero-voltage conversion pulse width modulated bidirectional DC-DC lift converter. Efficiency is improved by using ZVS and zero current switching (ZCS). The main features of the proposed converter are a simple control, a simple structure, and reduced stress on the power switch. However, the requirements for active and passive components are quite high. Reference [18] describes a new secondary buck–boost converter with continuous input and output currents, which is suitable for

renewable energy applications. However, for very high voltage boost requirements, the gains mentioned in this paper may still be insufficient, requiring a further increase in the complexity of the converter or the adoption of other techniques to increase the voltage gain. Reference [19] proposes a new bidirectional buck–boost converter topology designed to reduce power loss and consume right half plane zeros. This topology reduces the current stress on the inductor path by introducing a capacitive auxiliary path, thus reducing the on-loss of the inductor's DC resistance and improving the conversion efficiency in buck and boost modes. In boost mode, the switch needs to withstand a voltage higher than the input voltage, which decreases the reliability of the component. Reference [20] describes a bi-polar buck–boost converter, which has both positive and negative load voltage polarities and a wide voltage gain range. The front-end secondary booster circuit effectively reduces the ripple of the input current, which helps to improve the stability and efficiency of the system. The converter uses only four switches, which reduces the complexity of the drive circuit and makes the control circuit simpler.

3.3. Bidirectional Cuk Converter

The bidirectional Cuk converter [21] is formed by connecting a diode D_1 in inverse parallel with the original power switch S_1 of the unidirectional Cuk converter, and connecting a power switch S_2 in inverse parallel with the original diode D_2. Its topology is shown in Figure 7, and it has three operating modes: forward transmission mode, reverse transmission mode, and alternating operating mode. In the alternating operating mode, the power switch and diode conduct current in turn during a switching cycle, and the average energy transfer direction depends on the average value of i_{L1} and i_{L2}. If the average value is positive, the transmission direction is from the U_1 side to the U_2 side, and vice versa.

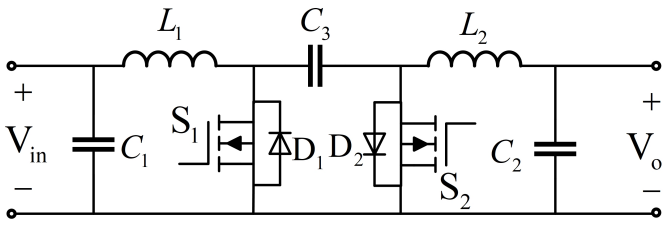

Figure 7. Topology of bidirectional Cuk converter.

The input and output of the bidirectional Cuk converter are inductors, which can reduce the current ripple, but there is no direct energy transfer path in its topology, and the energy can only be transmitted to the load through the capacitor first. This increases the circuit complexity, reduces energy transmission efficiency, and makes it unsuitable for high-power applications. The Cuk converter mentioned in the reference [22] adopts switched inductance and switched capacitance technology to improve the voltage boost capacity and reduce the voltage stress on the main switch.

3.4. Bidirectional Zeta/Sepic Converter

The input and output polarity of unidirectional Zeta and Sepic converters are the same. Since the topology of the bidirectional DC-DC converter formed by Zeta is exactly the same as that of the bidirectional DC-DC converter formed by Sepic, it is called the bidirectional Zeta-Sepic converter. Its topology is shown in Figure 8. The forward transmission is equivalent to the Zeta converter, the reverse transmission is equivalent to the Sepic converter, and like the bidirectional Cuk converter, in the alternating mode of operation, the direction of energy transmission is determined by the average current of the two inductors.

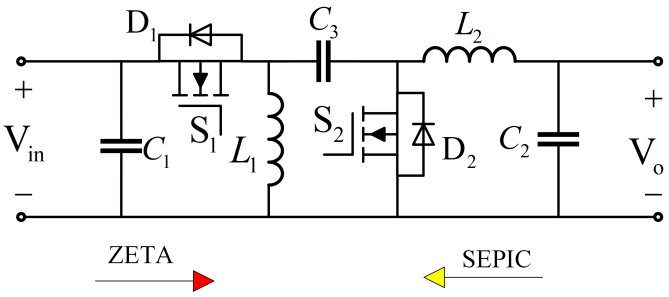

Figure 8. Topology of bidirectional Zeta/Sepic converter.

In the reference [23], the power semiconductor components of the Zeta-Sepic can be commutated by soft switches and operate under zero current switching ON and OFF, reducing ripple current and increasing voltage gain. Due to its cascading configuration, it is less efficient compared to other converters. Reference [24] describes a bidirectional zero-voltage conversion pulse-width modulation Sepic/Zeta converter, which combines Sepic and Zeta topologies and operates in Sepic mode during forward power flow and Zeta mode during reverse power flow. ZVS are implemented by introducing an auxiliary resonant circuit to reduce switching losses and improve conversion efficiency. Both the main switch and the diode are capable of ZVS operation, reducing losses caused by hard switching. Through synchronous rectification operation, the on–off loss is further reduced. Although the converter is more efficient at full load, it is less efficient under light load conditions due to the additional energy loss in the resonant circuit. ZVS operation at light load may also be less effective than at full load, resulting in loss of efficiency. The piece of reference [25] proposes a high-gain DC-DC converter based on Sepic, which is based on the traditional Sepic topology and increases the coupling inductance and two voltage multipliers to significantly improve the voltage gain. The voltage stress of the main switch is reduced by using a passive clamping circuit. By using a switch with low resistance, the on–off loss can be effectively reduced. In addition, due to the leakage of inductance and parasitic parameters of components, the effect of the soft switch is not ideal under a light load, resulting in increased energy loss. The converter proposed in reference [26] has the characteristics of a low output current ripple. By using coupling inductance technology and zero current switching, the efficiency is improved over the whole load range, and the current ripple cancellation circuit is introduced to achieve low output current ripple. Table 1 compares the characteristics of bidirectional non isolated DC-DC converters.

Table 1. Comparison of characteristics of bidirectional non-isolated DC-DC converters.

Reference	Features	Demerits	Efficiency	Power Density	Components and Complexity	Applications	Power
Buck/boost [14–16]	Simple structure, easy to design control and drive circuits, high conversion efficiency	Can only perform unidirectional boost or buck conversion, with inductance at the input or output terminals and large current ripple.	High	low	less	Low power, no need for electrical isolation, and only requiring unidirectional voltage regulation.	10 W or less up to 300 W

Table 1. *Cont.*

Reference	Features	Demerits	Efficiency	Power Density	Components and Complexity	Applications	Power
Buck–boost [17–19]	Capable of unidirectional voltage rise and fall conversion, with a simple driving circuit	Produces negative output	low	low	Less	Smartphones, iPads and laptops	10 W or less up to 300 W
Cuk [22]	The input side inductor acts as filter to prevent large harmonics	Polarity reversal in between input and output voltages	low	Moderate	more	Charging batteries, Electric vehicles	up to 500 Watts
Zeta-Sepic [23,24,26]	Compared to bidirectional Cuk, the input and output polarities are the same	Adding capacitors to the circuit path requires multiple energy conversions, resulting in low conversion efficiency and complex structure	low	Moderate	more	Application of high current output terminal batteries	up to 500 Watts

Table 1 is a comparative overview of the bidirectional DC-DC converter topology.

3.5. High Gain DC-DC Converter with Switched Capacitor/Inductor Boost Unit

The so-called boost unit involves combining the capacitor or inductance element with the function of energy storage and energy release and the diode or switching tube, through the one-way conductivity of the diode or control the working state of the switching tube (on/off), changing the energy flow mode of the converter, and building a switching capacitor [27,28] or switching inductance module with the voltage boost function. According to the types of components included, the boost unit can be divided into the switching capacitance unit, switching inductance unit, and switching capacitance inductance unit.

3.5.1. Switched Capacitance Unit

The switching capacitor [29] unit is a topological unit that realizes high voltage boost based on the optimization and improvement in the charge pump technology. By utilizing the characteristics of capacitor energy storage and voltage non-sudden change, multiple capacitors are charged and stored in parallel during the energy conversion process of the converter, and the output voltage of a higher voltage level is obtained by series discharge. The most basic high-gain DC-DC converter topology with a switched capacitor unit is shown in Figure 9, where capacitors C_1 and C_2 and diodes D_1 and D_2 form a basic switched capacitor unit. When the switch tube S is on, the input voltage source V_{in} charges and stores energy to the inductor L, and the capacitor C_2 charges and stores energy to the capacitor C_1 through the diode D_2. When the switch tube S is disconnected, the inductor L and capacitor C_1 release energy to the output load R and the capacitor C_2 and C_o through diodes D_1 and D_o, thereby increasing the output voltage level of the converter and increasing the voltage gain of the converter [30].

Traditional non-isolated and isolated DC-DC converters have some limitations: isolated converters in low- and medium-power applications are limited by leakage induction; large size and other factors, non-isolated classic and derived boost converters in the high duty cycle area of voltage gain are limited and have poor performance. A single-switch super-gain DC-DC converter based on a switched inductance capacitor network is proposed in reference [31]. Compared to existing converters, the converter achieves ultra-high DC voltage gain with a minimal number of devices and significantly improved voltage gain over the entire duty cycle range, while having a lower ripple content of output voltage and current. Reference [32] proposes a novel high-voltage gain-switched capacitor con-

verter, which realizes adjustable high-voltage gain through the combination of multiple capacitors and switches. Compared with a Dickson-based switched capacitor converter, the voltage and current stress are limited effectively through phase-shift modulation and resonant loop design, thus reducing capacitance volume and on–off loss. Although the phase-shift modulation reduces the switching loss, the diode still needs to withstand a large current stress.

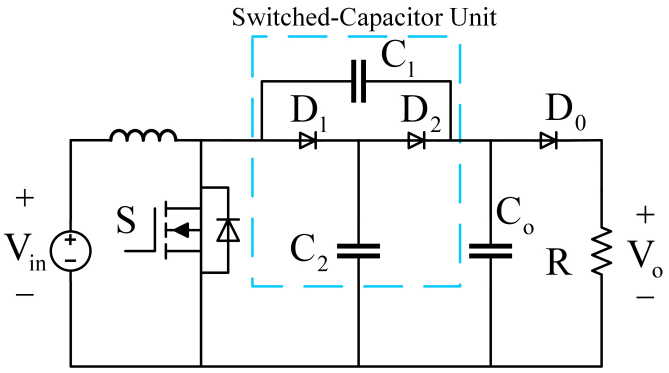

Figure 9. Topology of basic high-increment DC-DC converter with switched capacitor unit.

3.5.2. Switching Inductance Unit

Similar to the switched capacitor converter, the design of the switched inductor is based on the characteristics that the inductor current cannot change and the inductor has the energy storage function. In operation, the two inductors are charged in parallel to store energy, and the energy is released in series discharge to obtain higher voltage gain. Figure 10 shows the topology of a high-gain DC converter with a basic switching inductance unit, where inductors L_1, L_2 and diodes D_1, D_2, D_3 form the most basic switching inductance unit. It can be seen from the figure that when the switch tube S is switched on, the inductance L_1 and L_2 are charged and stored in parallel with the input voltage source V_{in} via diode D_1 and D_3, respectively. When the switching tube S is disconnected, the inductors L_1 and L_2 are connected in series to the input voltage source V_{in} via diode D_2, and the energy stored on them is released to the load R and the capacitor C_o via the output diode D_o.

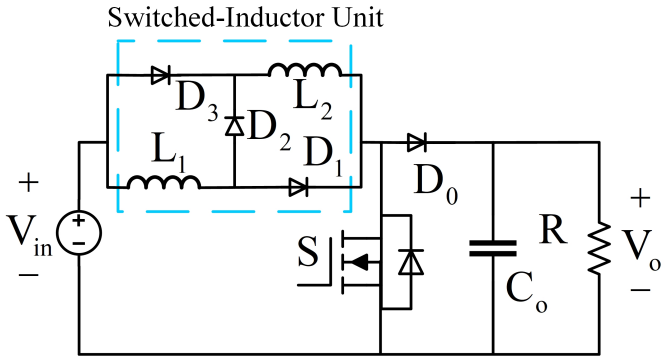

Figure 10. Topology of basic high-gain DC converter with switched inductance unit.

Compared with the traditional boost converter, the high-gain DC-DC converter with switched inductance unit flows through the inductor L_1 and L_2 shunt when the main switch tube S is switched on, and the inductor current per phase is smaller, thus reducing the volume and loss of the magnetic component and improving the output power of the converter. At the same time, the voltage gain of the converter is improved by the energy storage characteristic of the inductor. However, the high gain DC converter with switching inductance unit has the same defect as the traditional boost converter: the switching tube

works in the hard switching state, which increases the on–off loss. The reverse recovery loss of the output diode is large. Reference [33] proposes an improved switched inductance boost converter, which uses the principle of parallel charging and series discharge of reactive elements to achieve high voltage. By using two active switches to share the output voltage, the voltage stress of each switch is reduced. This design allows switching devices with low voltage ratings to be used, reducing device costs. By reducing the voltage stress on the switching device, the power loss of the switching device is reduced. Due to the use of multiple active switches, the overall switching loss is still present, especially at high-frequency operation, where the switch rise time and fall time introduce additional losses. The converters mentioned in reference [34] are suitable for renewable energy applications, especially photovoltaics. Compared with traditional DC-DC converters, the converter maintains the same number of semiconductor devices while reducing the number of passive components, thus improving the compactness of the converter and reducing the system cost. In addition, the converter has a higher gain.

3.5.3. Switching Capacitor Inductance Unit

A capacitor element is introduced into the switched inductance unit. The topology of the basic high-gain DC converter with switched capacitance-inductance unit is shown in Figure 11. The diode D_2, which is directly connected between the inductance L_1 and L_2, is replaced with capacitor C_1. The circuit structure can further improve the voltage boost capacity of the switching inductor unit by using the characteristics of capacitor storage and capacitor voltage non-sudden change. However, similar to the previous two high-gain DC converters with boost cells, the voltage stress of the switching device and the reverse recovery loss of the output diode are still large, which increases the working loss of the converter.

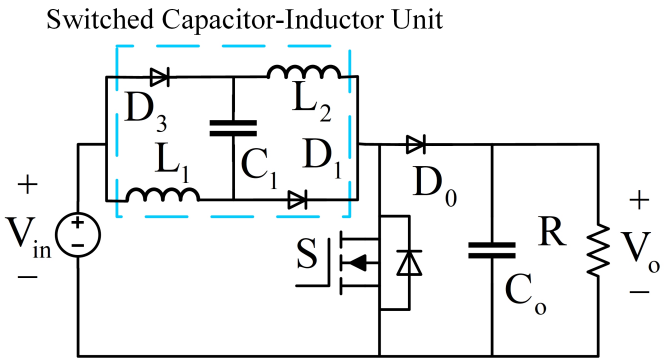

Figure 11. Topology of the basic high-gain DC converter with switched capacitor and inductance units.

The converter mentioned in reference [35] has the topology of switching capacitance and switching inductance, and the voltage gain is improved by inductance capacitor unit. Compared with conventional boost converters, this structure reduces the ripple of the input current and improves the efficiency and stability of the system. Reference [36] describes an improved hybrid switching inductor/switching capacitor DC-DC converter with a proposed structure with higher voltage gain at low duty cycle compared to conventional SL or SC converters. By adding an auxiliary switch, especially for high voltage gain, efficiency is improved. Reference [37] introduces the design and implementation of a high-boost DC-DC converter with active switching inductance and coupled inductance. By introducing active switching inductance and coupled inductance, the voltage stress on the power switch is effectively reduced. The voltage stress of the power switch is only a multiple of the input voltage, which greatly reduces the requirements for switching devices compared with traditional boost converters. However, the voltage stress on the diode is still high.

Through the combination of coupled inductors and multiple diode–capacitor networks, the voltage conversion ratio is significantly improved, and as the duty cycle increases further, the efficiency begins to decline, which requires a trade-off between voltage gain and efficiency. In summary, the booster unit constructed by capacitive/inductive energy storage can effectively improve the voltage gain of the converter, reduce the voltage stress of the switching device, and improve the efficiency of the converter. However, in high voltage gain applications, multiple switched capacitor/inductor boost units must be combined in series or in parallel, which increases the converter cost, which requires a trade-off between high gain and cost.

3.6. Coupled Inductance Converter

Magnetic coupling is one of the most popular voltage converter technologies recently, and the principle of transformer is the same, the coupling inductance is equivalent to a non-isolated transformer; in theory it can be regarded as a transformer with a certain coupling coefficient. By changing the turn ratio of the coupling inductance reasonably, the high voltage output of the converter is realized on the premise of avoiding the limit duty cycle. Figure 12 shows the basic topology of coupled inductance type high-gain DC converter [38]. When the switch tube S is on, the secondary winding voltage of the coupling inductor $V_{n2} = -\mathrm{N}V_{in}$; when the switch S is off, the secondary winding voltage is $V_{n2} = -\mathrm{ND}V_{in}/(1-\mathrm{D})$, where N is the ratio of turns of the primary and secondary winding of the coupling inductor. Ignoring its leakage inductance effect, the voltage gain of a high-gain DC converter with coupled inductance can be expressed as $\mathrm{M} = \frac{(1+ND)}{(1-D)}$.

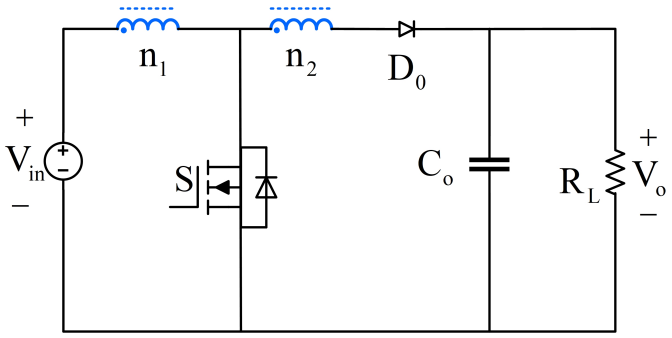

Figure 12. Basic topology of high-gain DC-DC converter with coupled inductance.

In boost technology, coupling using two inductors is the most commonly used technique, which reduces the components in the same voltage circuit and is easier to solve. However, the use of coupled inductors leads to the leakage inductance problem, which is a problem that needs to be considered. In addition, appropriate measures should also be taken to recover the energy stored in the leakage sensor, otherwise it may cause serious energy loss in the circuit. The converter proposed in reference [39] is composed of a set of coupled inductors and a switched capacitor network to achieve a 15-fold high voltage gain. The passive clamp circuit is used in the primary winding to recover the leakage energy, improve the output voltage, and solve the leakage problem. The converter mentioned in reference [40] uses tapped inductors as the front end of the low voltage energy generation system. Leakage sensing is integrated into the resonant groove, reducing the number of components. By using a boost capacitor in series with the secondary windings of the tapped inductor, a high voltage gain is achieved at the low turn ratio of the coupled inductor. By integrating the resonant passive clamp circuit, not only the voltage spike on the transistor is limited, but also the zero-voltage switching of the transistor and the zero current switching of the diode are realized. Resonant operation results in low power losses in the switch, providing high efficiency over a wide range of output power. Reference [41] describes a

high-voltage gain single-switch DC-DC converter with efficient leakage energy recovery function. The efficient recovery of leakage energy is an important requirement for such converters with coupled inductors to overcome high voltage stresses on semiconductor devices. The converter can effectively recover the leakage energy of the coupling inductor to the load through a passive clamping circuit. Therefore, the efficiency of the converter is greatly improved. The converter has lower diode voltage stress, and also improves the reverse recovery performance of the output diode. The converter proposed in reference [42] uses coupling inductors and voltage multipliers, which can achieve high voltage gain at low duty cycle. The main side adopts a staggered mode to reduce the source current wave. The converter primary switch has an active clamp auxiliary resonant circuit, which is used for soft switching and reduces switching loss. The voltage quad circuit provides ZCS with the ability to turn off all diodes, significantly reducing the voltage stress on all MOSFETs and diodes. It is summarized that these improved converters can not only flexibly increase the voltage boost capacity of the converters, but also effectively reduce the voltage peak caused by the leakage inductance of the coupled inductor and the parasitic capacitor resonance of the switch, and reduce the voltage stress of the switch tube. The switching tube works in the soft switching state, effectively reducing the switching tube conduction loss. At the same time, the voltage stress of the output diode is also reduced correspondingly, which is much smaller than the output voltage, and the reverse recovery loss is also significantly reduced. More importantly, the energy transfer is not affected by switching on and off during the normal operation of high gain DC converter with coupling inductance, and the magnetic core utilization of coupling inductance is high.

3.7. Cascade Converter

In the existing high gain implementation technology, the cascade converter boost technology is the simplest and most direct, the principle is to cascade two or more single-phase DC converters in turn (that is, the output of the upper level converter is the input of the next level converter), and finally get the total output voltage gain is the product of the voltage gain of all levels of the converter, that is, $M = M_1 \times M_2 \times \ldots \times M_N$, so as to achieve the purpose of improving the voltage boost capacity of the converter. Figure 13 shows the basic cascaded high-gain DC converter [43] built by cascading two traditional boost converters.

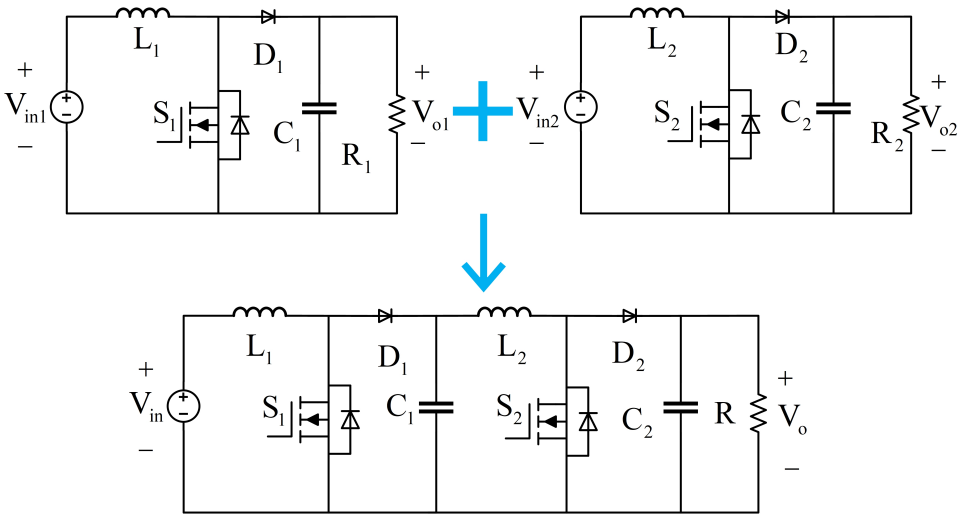

Figure 13. Topology of cascade converter.

Through analysis, it can be seen that when the duty cycle of the two switching tubes S_1 and S_2 of the converter shown in Figure 13 is the same, the voltage gain is $M = \frac{1}{(1-D)^2}$. In the pre-converter, the voltage stress of the switching device is small and the power consumption is small, while the voltage stress of the switching device of the post-converter is directly equal to the output voltage, resulting in a large switching loss and a large reverse recovery loss of the output diode. From the perspective of output power, all the switching devices in the cascade converter work in the hard switching state, and the equivalent on-resistance is relatively large, which increases the converter loss. Moreover, the energy is transferred and converted through the cascade unit layer by layer, and the loss level increases, resulting in the final efficiency of the converter system is low. Therefore, the cascaded high-gain DC converter is not suitable for the application of high voltage gain and high power density. In view of the above problems, reference [44] increases the output voltage by increasing the duty cycle. By recovering leakage energy, it helps reduce voltage spikes on the power switch. The coupling inductor is used to replace the aluminum foil inductor of the second booster stage, and the voltage multiplier is added to the secondary winding of the coupling inductor to further improve the voltage gain. When the duty cycle and turn ratio are 0.57 and 1, respectively, the voltage gain is about 22. Compared with the traditional secondary boost converter, the proposed converter is more efficient. In addition, in order to improve the converter efficiency, an optimal intermediate voltage tracking method is proposed in reference [45]. The intermediate voltage is adjusted by the duty cycle of the front and rear converters. In addition, the intermediate voltage range is determined by calculating the overall loss of the system, which improves the control speed of the algorithm. The experimental results show that the efficiency of the proposed control method is 2% higher than that of the uncontrolled condition. A novel passive lossless clamping circuit consisting of two capacitors and a diode is proposed in reference [46]. One capacitor of the circuit is used to construct the flow path of the leaking inductive energy, and the other is used to store the leaking energy. Compared with the classical passive lossless clamping circuit, the new circuit structure is more flexible and the number of additional components remains the same.

In summary, the cascaded converter is more suitable for small and medium power levels, and needs to be used with other high-gain realization technologies in high-power high-gain situations.

3.8. Interleaved Converter

For the improvement of the high gain DC converter, interleaving parallel technology [47] can effectively reduce the current stress of switching devices. The essence of the staggered parallel technology is to parallel the input inductors of multiple multiphase DC converters, and reduce the current stress of the switching devices of the converters by various shunt methods. The DC converter improved by interleaved parallel technology is more suitable for high-power applications. The interleaved converter topology is shown in Figure 14.

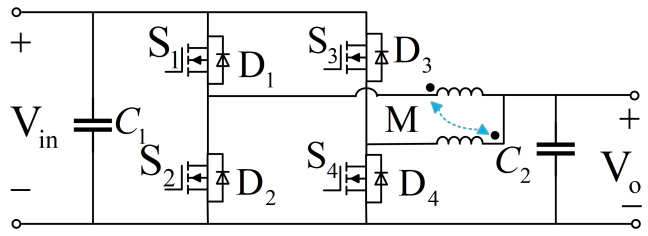

Figure 14. Topology of interleaved converter.

In reference [48], two coupled inductors and clamping circuits are added to the interlaced boost converter to achieve the ZVS condition when the switch is on and the ZCS condition when the diode is off, so as to generate the linear current of the switch and the diode. However, the converter relies on coupling inductance to realize soft switching, which limits the application of soft switching technology in high-voltage gain DC-DC converter. Reference [49] describes a high-gain compact interlacing boost converter that reduces the number and size of components by using coupled inductors and shared clamp capacitors. The leakage energy of the coupling inductor is effectively utilized, which further improves the converter efficiency and reduces the loss. However, under light load conditions, the efficiency will decrease due to the on–off and on–off losses that still exist. Especially when the input voltage is low, the leakage energy utilization is insufficient, which may affect the efficiency. The converter mentioned in reference [50] achieves very high voltage gain by coupling inductors and voltage multiplication units. The topology uses a staggered structure, and the input current ripple is significantly reduced. The reverse recovery problem of the diode is alleviated, and the lost energy is recovered. At the same time, coupled inductors and voltage multiplication units are used to achieve staggered energy storage at the output end, which reduces the voltage stress on the diode and switch tube. The converter does not need an extreme duty cycle or high turn ratio to obtain a higher boost voltage gain, and the turn ratio can be increased to obtain further voltage gain. Table 2 below compares the high gain converter efficiency, voltage gain and duty cycle, and cost, and produces an image of the voltage gain increasing with the duty cycle as shown in Figure 15.

Table 2. Compares the high gain converter efficiency, voltage gain and duty cycle, and cost.

Reference	Maximum Efficiency	Voltage Gain	Switching Tube	Diode	Capacitance	Inductance	Coupling Inductance
[44]	-	$\frac{(2N+1+D+N(1-D))}{(1-D)^2}$	2	5	5	4	2
[45]	95.23%	$\frac{(1-D_1)}{(1-D_2)}$	2	2	3	2	0
[46]	94.4%	$\frac{(2+N+ND)}{(1-D)^2}$	1	6	0	0	0
[39]	96.9%	$\frac{(1+2N+3D)}{(1-D)}$	1	4	5	0	1
[40]	96%	$\frac{(N+2)}{(1-D)}$	1	3	3	2	1
[41]	95%	$\frac{(2KN)}{(1-D)^2}$	1	5	4	1	1
[42]	90%	$\frac{4(N+1)}{(1-D)}$	4	4	6	0	2
[33]	97.17%	$\frac{(1+D)}{(1-D)}$	2	3	1	2	0
[34]	93%	$\frac{(3+D)}{(1-3D)}$	2	7	3	2	0
[35]	96%	$\frac{(3+D)}{(1-D)}$	1	7	4	2	0
[36]	92.64%	$\frac{(5D_1-D_2+3)}{(1-D_1-D_2)}$	3	10	4	3	0
[31]	91.2%	$\frac{(2-D)}{(1-D)^2}$	1	4	3	2	0

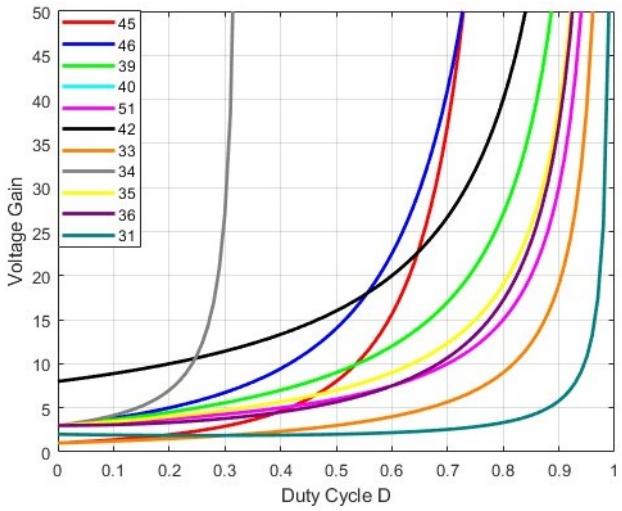

Figure 15. Voltage gain and duty cycle curves.

3.9. Multilevel Converter

The multilevel converter can control the series output of different DC power supplies through the specific topological transformation of multiple DC power supplies and power electronic devices. Under different switching states of the conversion circuit, the multilevel output of different amplitudes can be obtained at the output end. Because there is no inductance, the weight and size of the converter are significantly lower than those using magnetic components, so the converter is compact and low cost. Common multilevel topologies are divided into three types: diode clamped (NPC), flying capacitor (FC), and H-bridge cascade. Each of these three structures has its own characteristics, but there are also corresponding shortcomings. Their topology is shown in Figure 16. For example, compared with other multilevel converters, the H-bridge cascade topology has advantages such as low voltage stress, multiple redundant switching states, flexible control mode, easy encapsulation, and easy expansion of level number. However, the disadvantage is that multiple independent power supplies or multi-winding phase-shifting transformers are required, which is large and costly.

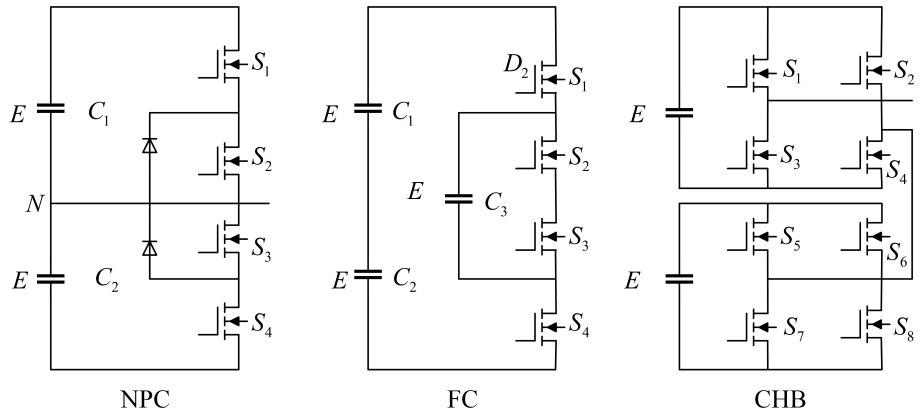

Figure 16. Basic topology of multilevel converter.

Reference [51] describes a high gain ratio modular multilevel DC-DC converter, which is based on the standard boost converter topology, but replaces a single switch with multiple capacitor clamp modules, operates in the resonant mode, and achieves efficient operation through phase-shift pulse-width modulation control. Due to the use of multiple capacitor clamp submodules, although the voltage gain is improved, the voltage stress on each submodule is higher, and the diode current stress on the secondary side is larger, resulting

in increased diode loss. Under light load conditions, resonant current and switching loss are significant, which affect the overall system efficiency. Reference [52] describes a modular multilevel DC-DC buck–boost converter derived from the traditional switching mode converter. This topology combines the concept of modular multilevel converter and presents a step-up converter suitable for HVDC systems. Compared with the traditional dual active bridge converter, the converter has lower loss and lower magnetic component requirements. Because the converter adopts multilevel topology, the current ripple is large, which puts forward higher requirements for the subsequent filter circuit, and may need to increase the design cost of the filter. Reference [53] describes a novel modular multilevel DC-DC converter with characteristics similar to a flying capacitor converter, called a current-shaping modular multilevel forward converter. The converter is designed to achieve high power density and is suitable for applications from medium voltage DC networks to low voltage DC loads. Although the design reduces the current of the voltage source module in series through modularization, the voltage source module capacitors and switching devices still bear higher voltage stress under the condition of a higher conversion ratio. With the decrease in the output voltage, the voltage stress of the module increases, especially the forward voltage drop of the diode significantly affects the efficiency. Reference [54] proposes a new type of multilevel press payment, which is suitable for renewable energy applications. The structure has 3 unequal input sources and 10 switches, which can produce 15 output voltages, and more voltage levels can be added by cascading. Based on level control, the harmonic distortion of the output voltage and current is very low, which can produce high-quality output voltage.

4. Isolated Bidirectional DC-DC Converter Topology

4.1. Flyback Converter

The bidirectional flyback converter is formed after the reverse parallel diode on the primary side power tube of the unidirectional flyback converter [55] and the reverse parallel power tube on the secondary side diode. The topology is shown in Figure 17, and it can work in forward transmission, reverse transmission and alternating transmission modes. Like the bidirectional forward converter, there is no current discontinuous mode in alternating mode. It has the advantages of electrical isolation, simple topological structure, low cost, bidirectional transmission, etc., and is suitable for low power applications. However, compared with the bidirectional forward converter, the power device may bear larger voltage and current stress, and the energy on the transformer leakage induction cannot be transmitted to the secondary side through the coil, and the current generated by these energies will resonate with the power tube capacitance, resulting in voltage spikes, which may break down the power tube.

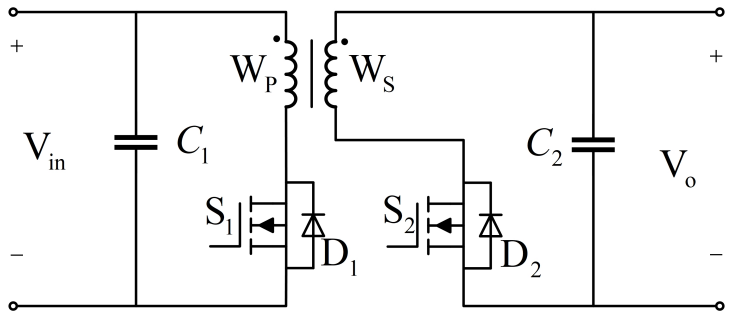

Figure 17. Topology of bidirectional flyback converter.

The flyback converter switch tube needs to withstand the high voltage caused by leakage induction during the blocking period, in order to reduce voltage stress, it is generally necessary to add clamping circuit. Clamping circuits can be roughly divided into passive clamping circuits and active clamping circuits. The classic passive clamp circuit uses resistive- capacitive-diode (RCD) structure, which transfers the leaky energy stored in the flyback transformer to the clamp capacitor and then consumes it in the form of heat energy. Although this method reduces the voltage stress of the switching tube, the energy in the leakage induction is not utilized, and the converter efficiency is not high. A flyback converter with a non-complementary active clamp control method is proposed in reference [56]. The active clamp circuit can reduce the voltage stress of the main switch and allow the leakage energy recovery at the same time, so that the converter can achieve high efficiency under a heavy load and light load. The converter mentioned in reference [57] has a clamping circuit for leakage energy recovery and charging the clamping capacitor to improve voltage gain. In addition, all switching tubes operate under soft switching conditions, and the diodes use soft commutation. Reference [58] discusses a bidirectional flyback converter based on an RCDD buffer. The advantages of this converter are its simple structure, good isolation performance, small number of components and controllable dynamic behavior. The buffer reduces ringing and loss by reducing voltage spikes caused by transformer leakage and absorbing leakage energy. In the step-down mode, the current of the secondary diode is prone to overshoot, which increases the switching loss. In addition, IGBT will be subjected to higher voltage and current stress during the ups and downs mode conversion. RCD buffers and active clamping circuits can be used to suppress these voltage spikes, but clamping operation of RCD buffers increases power consumption, while active clamping requires additional power switches. In order to solve these problems, a design method of quasi-resonant flyback converter with partial voltage resonant capacitor is proposed in reference [59], which reduces voltage spikes and improves power conversion efficiency. In order to achieve the high performance of the flyback converter, soft switching technology can be applied to the main switch. Reference [60] introduces a ZVS-based staggered flyback converter, which consists of two parallel flyback converters and realizes zero-voltage switching through an auxiliary inductor in parallel between two rectifier diodes. The ZVS feature reduces voltage spikes during switching operation and reduces switching device losses. Although ZVS technology reduces switching losses, zero voltage switching is difficult to achieve under light load conditions. Interleaved flyback converters can be used in high power situations. Reference [61] describes an interleaved boost/flyback converter with self-balancing interleaved output current without current or voltage control loop. Coupling inductors and SC are used to achieve high voltage gain in the topology, and the maximum gain of the converter can also be extended by adjusting the turns ratio of the coupling inductors.

4.2. Forward Converter

The bidirectional forward converter [62] is composed of parallel diodes at both ends of the primary side power tube and parallel power tubes at both ends of the secondary side of the unidirectional forward converter. The topology is shown in Figure 18, which can work in forward transmission, reverse transmission and alternating transmission modes. In this topology, S_1, S_2 and S_3 all work in PWM control mode. S_1 and S_2 are switched on and off at the same time, and work in a complementary manner with S_3. The bidirectional forward converter has a simple working principle, easy design of its control and drive circuit, which is suitable for small and medium power occasions, but the transformer used is in a unidirectional excitation state, and the utilization rate is low.

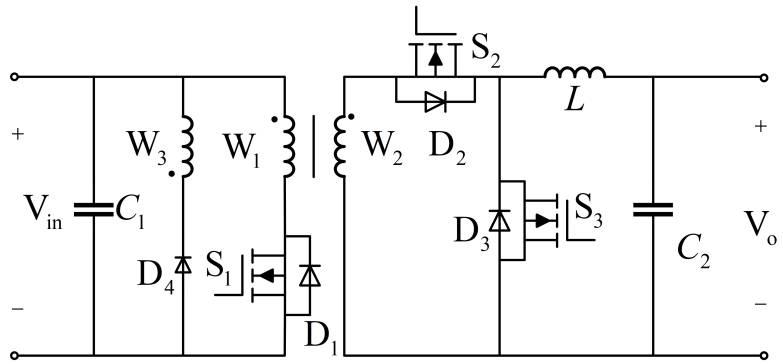

Figure 18. Topology of bidirectional forward converter.

The magnetic reset of transformer is a special problem of forward converters. The characteristics of forward converters are different with different magnetic reset modes, and the range of the duty cycle is also different. Two-switch forward converters are widely used because of their robustness, but they also have two disadvantages, the inherent hard switching topology and the input voltage used for transformer reset, and the maximum duty cycle is limited to 0.5. To solve the above problems, reference [63] proposes a double-switch forward converter with reset windings and an auxiliary active clamp circuit suitable for wide input voltage range. The converter provides a simple reset scheme through the reset windings, while maintaining low voltage stress on the switch, so that the duty cycle can exceed 0.5. In addition, the magnetized inductance is designed properly, which can realize the zero voltage switch of the main switch by using the active clamp network.

The structure of the RCD forward converter is shown in the Figure 19. Because the clamping capacitor C_c is large, it can be regarded as a voltage regulator in stable operation. When the switching tube is turned off, the diode D_c is switched on, and the voltage on the C_c makes the transformer magnetic reset. It has the advantages of simple circuit structure and low cost. However, the excitation energy and leakage energy of the transformer are completely consumed in the reset resistance, and the conversion efficiency is low, which is suitable for applications with low efficiency requirements and low price [64].

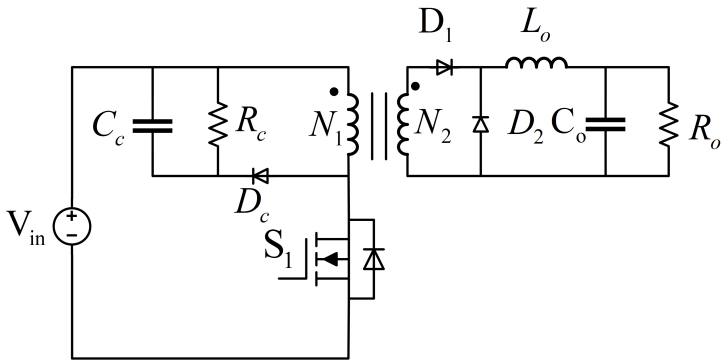

Figure 19. RCD forward converter structure.

The structure of the active clamp forward converter is shown in Figure 20. The main switching tube S_1 is turned off, the auxiliary switching tube S_c is switched on, and the voltage of the clamping capacitor C_c makes the transformer magnetic reset. Under certain conditions, the zero voltage of the main switch can be turned on, but at the cost of certain on-off loss. The excitation energy and leakage energy of the transformer are both returned to the input source, and the conversion efficiency is high. The magnetic core of the transformer is bidirectional magnetized, and the magnetic core utilization rate is high. However, the circuit and drive are more complex, and the circuit cost is higher.

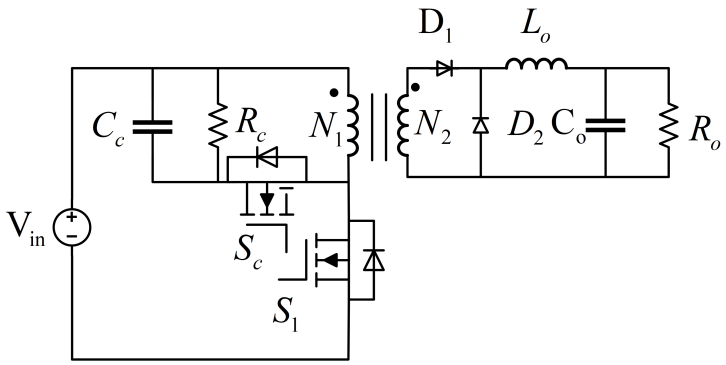

Figure 20. Structure of active clamp forward converter.

The converters mentioned in reference [65] use single switches and resonant converters, which reduce the cost and complexity of the circuit. The load current is evenly distributed between the inductor and the switch, which equates to an increase in power conversion efficiency. A staggered active clamp forward converter is proposed in reference [66], which can achieve high efficiency without adding any additional components. By rearranging the components on the active clamp forward module, the module can accommodate high input voltages, significantly reducing the primary conduction loss due to the transformer's large turn ratio and the extended duty cycle at the rated input voltage.

As shown in Figure 21, the resonant magnetic reset forward converter topology [67] realizes the magnetic reset of the transformer by using the parasitic capacitor of the switching tube or the shock of the external shunt capacitor of the drain-source pole and the excitation inductance of the transformer. Under the same duty cycle, the switching tube voltage stress of the resonant reset forward converter is higher than that of the RCD forward converter and the active clamp forward converter.

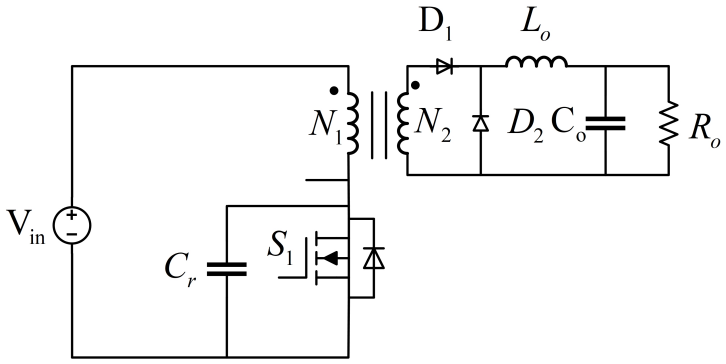

Figure 21. Resonant magnetic reset forward converter topology.

A novel self-driven synchronous rectifier single-switch forward converter controlled by variable magnetized inductance is proposed in reference [62], which provides a wide range of zero-voltage switching conditions. The leakage sensing of the transformer acts as a virtual inductor, transmitting power to the secondary side. Auxiliary capacitors are used with leakage and magnetized electricity to obtain ZVS conditions for the main switch and reset the transformer core. It does not contain additional reset winding and has the advantages of simple structure and low cost. In addition, the variable magnetizing inductance is realized by using DC bias winding.

4.3. Push-Pull Converter

The power switches connected in reverse parallel at both ends of the diode on the secondary side of the unidirectional push-pull converter form the bidirectional push-pull

converter shown in Figure 22, which can realize bidirectional energy transmission and alternating operation of inductive current. The transformer of the bidirectional push-pull converter also has leakage inductance, and the power switch is subjected to greater voltage and current stress, which makes it unsuitable for high-voltage environments with harsh conditions. However, its power level is higher than that of the bidirectional flyback converter.

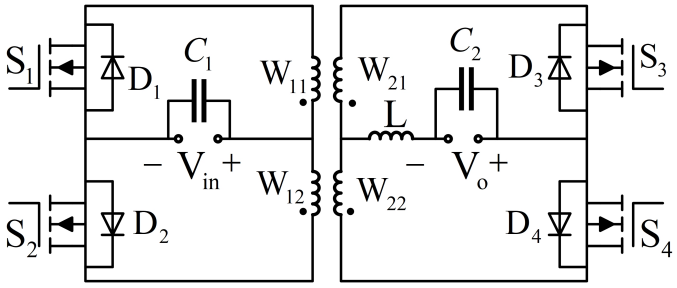

Figure 22. Push–pull converter topology.

Push-pull converters are favored for their simple structure and bidirectional excitation of transformers. However, this converter has some disadvantages, such as the energy stored in the drain inductor when the switch is off can cause voltage spikes, which are usually absorbed by the clamping circuit. A novel push-pull DC converter topology with complementary active clamping function is proposed in reference [68]. By adding a clamp capacitor between the active switches, the clamp voltage is maintained and the energy stored in the leakage inductance is restored. In addition, the topology expects the transformer to have a larger leakage inductance to buffer the energy transfer, and the rectifier diode to be able to conduct naturally. Three-switch push-pull full-bridge bi-directional DC/DC converters are used because they have fewer power switches and lower cost than dual active Bridges. However, it has the problem of high voltage stress and difficult to realize zero voltage switching under a full load. A single-switch push-pull full-bridge bi-directional DC converter is proposed in reference [69], which reduces the voltage stress of the power switch by adding a clamp capacitor between the active switches and facilitates device selection. In addition, the energy stored in the transformer leakage inductance is used for soft switching action without the need for additional resonant inductance. A push-pull DC converter based on active clamping is proposed in reference [70]. The push-pull structure with a single input inductance can effectively reduce the input current ripple. The voltage stress on the power switch can be limited by active clamping technology, so that the power switch with a lower resistance value can be selected to reduce the on-loss hybrid manufacturing cost. Because there is no circulating current, the energy loss of ZVS involved in the active clamp circuit is less than that of traditional resonant methods. It also has some shortcomings, such as the voltage oscillation of the secondary diode parasitic capacitor, the small range of the converter to transmit energy to the output and the relatively large current ripple at the output, which needs to be further improved. Reference [71] proposes a new push-pull DC-DC converter that maintains the clamp voltage and recovers the energy stored by leakage sensing by adding a clamp capacitor between the active switches. By using the leakage buffer energy transfer of the transformer, the switch realizes self-clamping and has natural soft switching characteristics. In addition, the rectifier diode naturally reverses and has no reverse recovery problems. However, due to the large leakage inductance, the voltage stress of the switching tube is twice that of the input voltage, which can lead to device selection limitations and cost increases in high voltage applications.

4.4. Half-Bridge Converter

A bidirectional half-bridge converter is formed by inverting parallel power tubes on two diodes on the secondary side of the half-bridge converter [72], and its topology is shown in Figure 23. Because of its simple structure and fewer required devices, it is suitable for small and medium power applications. Zero voltage switching of all switching devices can be achieved by single phase shift control without auxiliary devices. The switching loss is reduced to a certain extent, but the transformer is in a unidirectional excitation state and the utilization rate is low. Because the transformer is in the phase shift control mode, it is not suitable for applications with a large voltage regulation range.

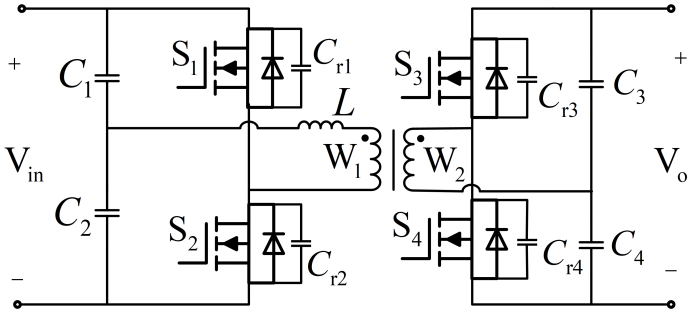

Figure 23. Topology of half-bridge converter.

Reference [73] proposes a ZCS current-fed full-bridge PWM converter with adaptive soft-switch buffer energy, which uses a simple buffer composed of two unidirectional switches and a capacitor to realize soft-switch operation over a wide line and load range. All primary switches use zero-current switches and buffer switches use zero-voltage switches. The energy used for the soft switch is adaptive. The implementation of ZCS relies on phase shift control, which results in a loss of duty cycle for the converter. Although the design reduces the loss through optimization, the duty cycle loss still limits the adjustable range of its voltage gain compared to conventional hard switching converters. Literature [74] addresses the problems of poor output voltage regulation and low conversion efficiency of full-bridge series resonant converters under a light load. A dual-mode control strategy is proposed, which realizes ZVS and low switching noise. In reference [75], the medium converter can reduce the rated power of the photovoltaic system and improve the efficiency of the photovoltaic system. The efficiency curve of the converter remains flat across a wide range of photovoltaic module voltages and all load ranges, but the derived two-port converter can only achieve voltage boost. Reference [76] describes a current feed converter using a quasi-Z-source network. Due to its inherent lift and clamp functions, the proposed converter can effectively eliminate the problem of starting and switching voltage overshoot. In addition to this, compared with conventional converters, the switching current stress is reduced and the switching devices are reduced.

4.5. Full Bridge Converter

Oppositely parallel four power tubes on the four diodes on the secondary side of the unidirectional full-bridge converter form a bidirectional full-bridge converter, as shown in Figure 24. Compared with the bidirectional half-bridge converter [77], the bidirectional full-bridge converter has a complex structure, requires more devices, and increases the volume and design cost of the product, but the current stress of the power device is only half of it, which is suitable for occasions with higher power levels. If the clamp circuit is added to the converter, it can ensure that the power tube all works in the soft switching state.

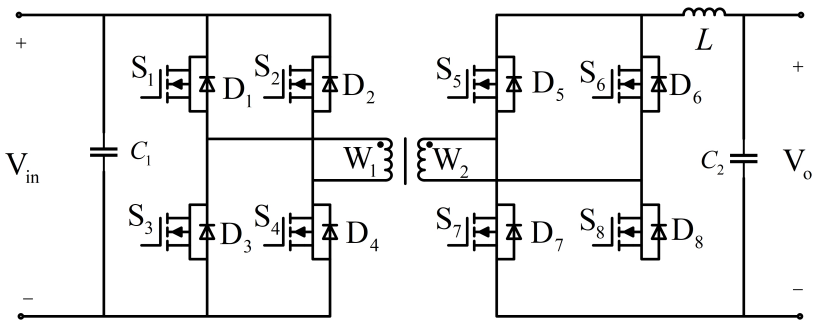

Figure 24. Topology of full-bridge converter.

Reference [78] proposes a ZCS current-fed full-bridge PWM converter with adaptive soft-switch buffer energy, which uses a simple buffer composed of two unidirectional switches and a capacitor to realize soft-switch operation over a wide line and load range. All primary switches use zero-current switches and buffer switches use zero-voltage switches. The energy used for the soft switch is adaptive. The implementation of ZCS relies on phase shift control, which results in a loss of duty cycle for the converter. Although the design reduces the loss through optimization, the duty cycle loss still limits the adjustable range of its voltage gain compared to conventional hard switching converters. Literature [79] addresses the problem of poor output voltage regulation and low conversion efficiency of full-bridge series resonant converters under light load. A dual-mode control strategy is proposed, which realizes ZVS and low switching noise. In reference [80], the medium converter can reduce the rated power of the photovoltaic system and improve the efficiency of the photovoltaic system. The efficiency curve of the converter remains flat across a wide range of photovoltaic module voltages and all load ranges, but the derived two-port converter can only achieve voltage boost. Reference [81] describes a current feed converter using a quasi-Z-source network. Due to its inherent lift and clamp functions, the proposed converter can effectively eliminate the problem of starting and switching voltage overshoot. In addition, compared with conventional converters, the switching current stress is reduced and the switching devices are reduced.

4.6. Resonant Converter

The topology of the dual active bridge (DAB) converter is shown in Figure 25. DAB is the most representative and widely used isolated bidirectional DC-DC converter. The main control mode of the converter is phase shift control, which adjusts the output energy size and direction by controlling the phase shift angle between the primary and secondary switch tubes. Although the phase-shift control mode can realize the zero-voltage switching of the switching tube, it will also cause the problems such as the loss of reflux power and duty cycle. At the same time, when the converter works under light load, the switching tube will lose the soft switching characteristic, resulting in lower efficiency of the converter [67].

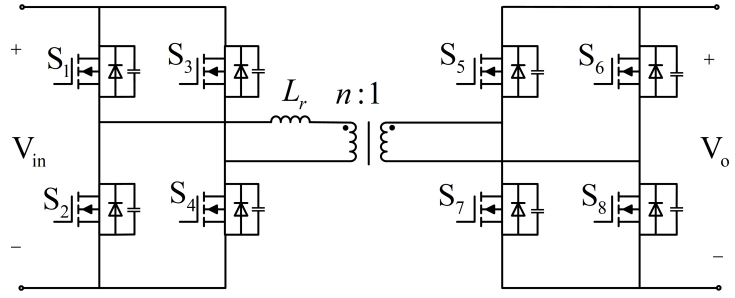

Figure 25. Dual active bridge converter topology.

Resonant DC-DC converter [82] has been widely concerned because it can realize the zero voltage on and zero current off of the switching tube and has high energy conversion efficiency. The resonant soft switch converter includes Inductor–Capacitor(LC) series resonant, LC parallel resonant, and Inductor–Inductor–Capacitor (LLC) resonant converter. Because the LLC resonant converter has great advantages over LC series resonant and LC parallel resonant converters in terms of voltage controllability and soft switching range, the LLC resonant converter is generally selected. Since the current of the DAB converter is a trapezoidal wave, the AC current amplitude of the DAB converter is smaller than that of the LLC converter at the same voltage and power, so the device current stress of the DAB converter is smaller than that of the LLC converter. The DAB converter can only realize the ZVS on of the switching tube, but not the ZVS off of the device.

The bidirectional LLC resonant converter is shown in Figure 26. It can realize the ZVS characteristics of the primary side switching tube and the ZCS characteristics of the secondary side switching tube, which can reduce the switching loss of the converter and improve the efficiency of the converter. However, in reverse operation, its equivalent circuit is the same as that of LC series resonant converter, which only has the function of reducing voltage, and the ZVS of the switching tube can be realized only under a heavy load [83].

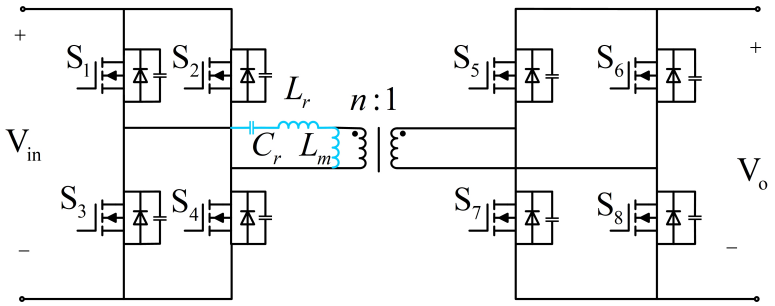

Figure 26. Bidirectional LLC resonant converter.

Based on the bidirectional LLC resonant converter, reference [84] constructs a bidirectional asymmetric CLLC resonant converter structure by adding a resonant capacitor C_{r2} to the transformer's secondary side, as shown in Figure 27. Compared with the converter in Figure 26, the converter is capable of voltage lifting and lowering during bidirectional operation. However, due to the asymmetry of the converter topology, the resonant frequency and gain characteristics of the converter are different in forward and reverse operation, and this difference will increase the difficulty of the converter parameter design and the complexity of the control.

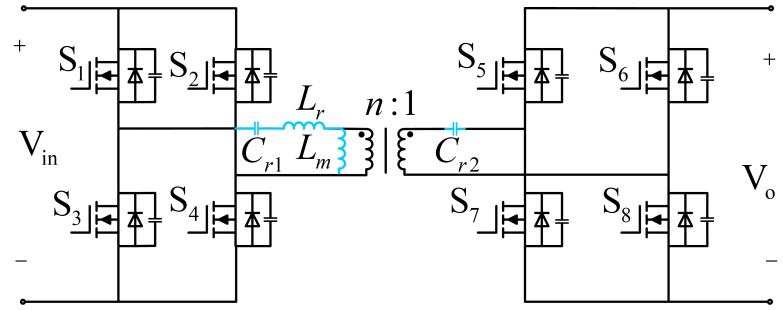

Figure 27. Bidirectional CLLC resonant converter.

On the basis of the converter in Figure 27, a symmetrical bidirectional CLLC resonant converter as shown in Figure 28 is formed by adding the secondary resonant inductor L_{r2}. Because of the symmetry of the CLLLC resonant converter, it works in the LLC resonant mode when the energy flows forward and backward, and can realize the ZVS of the energy

outflow side device and the ZCS of the energy inflow side device, and the voltage gain is greater than 1.

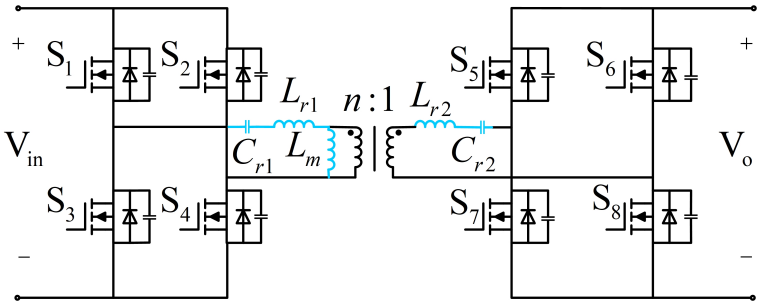

Figure 28. Bidirectional CLLLC resonant converter.

Literature [85] proposes an improved LLC resonant converter by adding two resonators on the primary side and a rectifier bridge on the secondary side to expand the output voltage range and improve the efficiency at medium and low output voltages. Through the control of pulse frequency modulation, zero voltage switching can be realized in the whole range, which improves the efficiency of low and medium voltage, and avoids the problem of large loop current and switching loss caused by traditional phase shift modulation. Due to the addition of additional magnetic elements and switching tubes, the power density of the whole converter is reduced, and the volume is increased, which is not suitable for the application scenarios with high power density requirements. Reference [86] proposes an improved bidirectional CLLC resonant DC-DC converter to improve efficiency in wide voltage range applications. The transformer adopts LC series resonant branches in parallel with the transformer, so that the equivalent inductance of the parallel branches and the equivalent excitation inductance of the transformer change with the change in the switching frequency. In this way, the converter can automatically adjust the operating frequency under different voltage gain requirements to reduce the switching current and cycle power at high frequencies and obtain a higher voltage conversion ratio at low frequencies. Due to the existence of parallel LC resonant branches, at high frequencies, large voltage stress will be generated on the primary side switch, and high-voltage resistant devices are required, which increases the cost. Reference [87] proposes a structurally reconfigurable series resonant DC-DC converter designed to address the challenges of wide input and configurable output voltages, especially for photovoltaic and grid-connected renewable energy systems. The basic principle, operation mode, characteristic comparison, design guide, and experimental verification of the converter are described in the reference. The converter realizes a wide input voltage range and two configurable output voltages by using bidirectional primary and secondary bridge circuits combined with fixed frequency PWM control. This design allows the converter to maintain low on-loss and high performance over a voltage gain range of 0.5 to 2 times. Despite the use of soft switching technology, the current stress of the secondary diode is large, which may lead to increased losses and heating problems. The primary switching tubes (S_3 and S_4) have higher current stress when switched off, especially when operating in the intermediate gain zone, which increases switching losses. Reference [88] proposes an isolated high-gain boost converter based on an active secondary side quasi-resonant loop to improve the efficiency and performance of DC-DC converters in high-gain applications. By placing the resonant circuit on the secondary side, the current stress and power loss of the resonant capacitor are effectively reduced, and the control of synchronous rectification is simplified. With these improvements, all switches and diodes achieve ZCS or ZVS with significantly less switching loss. Secondary side switches S_5 and S_6 are subjected to large voltage stress, and the peak voltage in the resonant process will be higher than the theoretical value, requiring the use of devices with higher voltage

levels, which increases the cost. Table 3 summarizes and compares the topology of the bidirectional isolated DC-DC converter.

Table 3. Comparison of bidirectional isolated DC-DC converter topologies.

Topology	Features	Demerits	Efficiency	Power Density	Components and Complexity	Applications	Power
Flyback [56–58,61]	Current isolation and good dynamic performance	High voltage stress	low	low	less	UPS and low power applications	10 W or less, up to 150 W
Forward [64,66,67]	Smaller transformer core	Snubber circuits are required to minimize the high voltage spikes	Moderate	Moderate	less	Low- and medium-power applications.	100–500 W
Push Pull [68,69,71]	Smaller transformer core but it is excited in both directions	Current ripples in input side and high voltage stress across switching devices	High	High	more	Medium and high power applications	500–1000 W
Half-bridge [73,74]	Less semiconductor devices	High voltage stress is limited to Vs	Moderate	Moderate	less	Medium power applications like fuel cells and batteries	500 W
Full-bridge [80]	Suitable for integrating applications	High voltage stress is limited to Vs	Moderate	High	more	Suitable for high power applications like electric vehicles and hybrid electric vehicles	2000 W
Resonant converters [82,83]	Suitable for multi-input multi-output integrating applications	High input current ripples and circulating currents	Moderate	High	more	Multi-port systems like PV, wind, batteries and energy storage systems	above 2000 W

5. Three-Port Converter

The three-port DC-DC converter is highly flexible and efficient in photovoltaic systems, capable of simultaneously connecting cells, photovoltaic panels and loads to achieve multi-directional power flow and stabilize output voltage and current through precision control algorithms. Its characteristics of multiple output voltages, space saving and strong adaptability enable it to effectively manage and optimize the distribution of photovoltaic energy, improve energy efficiency, and meet the needs of photovoltaic systems for multiple voltage outputs to ensure system stability and reliability.The topology of the three-active full-bridge DC converter is shown in Figure 29. In terms of the economy of the topology, such converters tend to utilize more components than other types of three-port converters, and the cost and volume increase accordingly. This kind of converter has the advantages of simple control and simple structure. The three-active bridge converter has three DC voltage ports, each DC port is connected to the three-winding high frequency transformer through a full-bridge switching network and an energy storage inductor, and each switching tube has an anti-parallel diode and parasitic capacitor, which is more convenient to reduce the opening loss of each switching tube of the converter on the basis of realizing phase shift control.

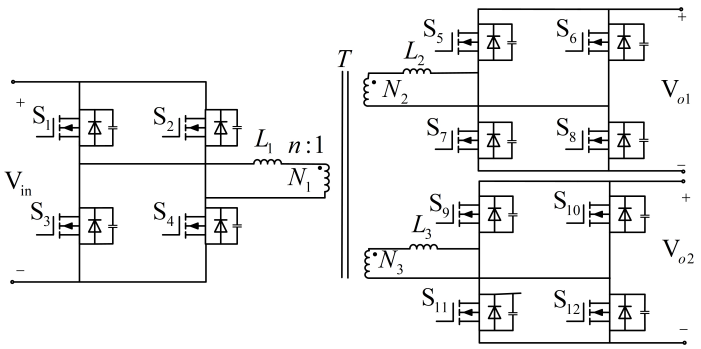

Figure 29. Three-active full-bridge DC converter topology.

The converter proposed in reference [89] improves the input/output voltage conversion ratio, provides a wider voltage control range, and reduces the voltage boost time of the converter. However, too many devices are required, and the volume is large, and the cost will be high. The converter mentioned in reference [90] adds a controllable free path, and realizes photovoltaic voltage regulation and battery charge management at the same time. By using flexible power flow regulation, photovoltaic panels and batteries can share load current adaptively, reducing the power conversion stage, and achieving a compromise between cost and efficiency. But when the power is increased, the efficiency decreases. The converter mentioned in Reference [91] adopts an LCL resonant circuit to realize the advantages of soft switch and a minimum number of switches of the main switch. It can track and control the maximum power point of the solar panel when there is solar radiation, and charge and discharge control of the battery when there is residual energy and insufficient power relative to the load. The voltage stress and di/dt value of the main switch are reduced. The converter proposed in reference [92] has the characteristics of reducing the number of switches and cost, and adopts hybrid modulation strategy to achieve wide DC voltage gain from PV to load, small input current ripple, and flexible power management between three ports.

6. Switch Conversion Strategy

The application of switching strategies in isolated bidirectional DC-DC converters is primarily reflected in the control of alternating conduction of bridge arm switches in DAB topologies.

6.1. Single-Phase Shift Modulation

Single-phase shift (SPS) modulation is the simplest control method [93], and its waveform is shown in Figure 30. When the DAB converter works, the switching frequencies of H_1 and H_2 bridges on both sides are the same, the diagonal switching tubes of the full bridge on both sides are switched on in turn, and the switching angle is 180°. The inverter output voltage of the full bridge on both sides is the square wave voltage with a duty cycle of 50%. By controlling the phase angle between the square waves, the magnitude and phase of the voltage at both ends of the inductor L_1 can be controlled, and then the magnitude and flow direction of the power can be controlled. It is suitable for the case of a small input and output voltage variation range, which can achieve high efficiency. When the voltage transmission ratio is equal to about 1, the modulation mode can realize zero voltage opening of all switching tubes and further improve efficiency. However, when the voltage transfer ratio is not equal to 1, the current stress and return power of the converter will increase correspondingly, and the soft switching range will also decrease, resulting in lower efficiency [94]. In order to improve the shortcomings of SPS, new shift concepts such as extended-phase shift (EPS), double-phase shift (DPS), and triple-phase shift (TPS) have been

proposed. By increasing the number of phase shift angles and changing the relationship between phase shift angles, the conversion efficiency of the converter is improved.

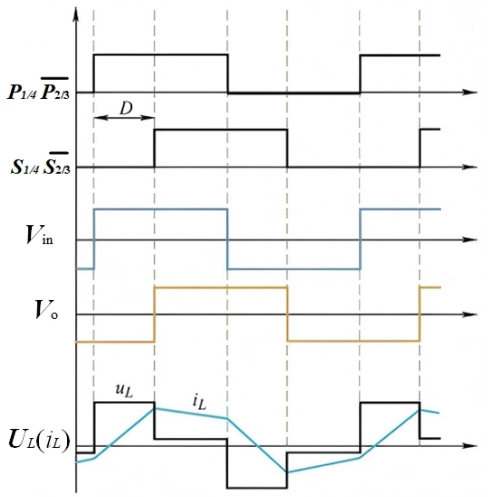

Figure 30. Single-phase shift waveform diagram.

6.2. Extended-Phase Shift Modulation

SPS will increase the current stress in the case of voltage mismatch, and some switching tubes will also lose the soft switching characteristics, because SPS control has only one degree of freedom, which is only used to control the transmission power, and cannot optimize the current stress. In this case, the efficiency and performance of the converter are limited. In contrast, the EPS modulation [95] increases the shift ratio inside the original side bridge, and the control freedom becomes two, which improves the flexibility of the converter control and provides more possibilities for converter optimizationand its waveform is shown in Figure 31. By adjusting the two shifts, the output characteristics of the converter can be more stable, and there is a larger soft switching range, which reduces the switching loss and improves the efficiency of the converter.

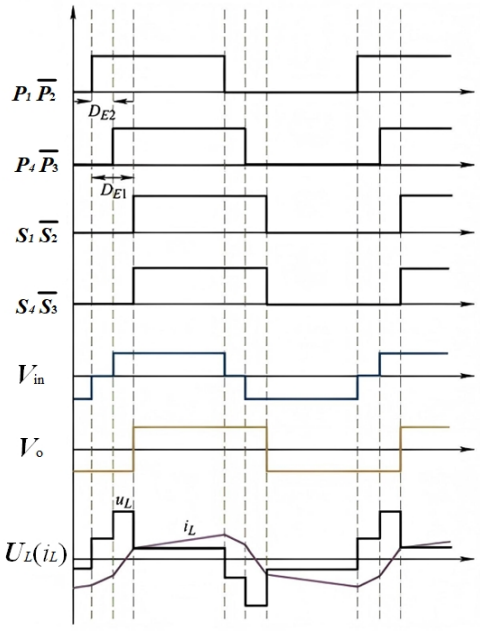

Figure 31. Extended-phase shift waveform diagram.

6.3. Double-Phase Shift Modulation

SPS can effectively reduce the backflow power and current stress of DAB converter to a certain extent. However, in practical applications, in order to ensure the consistency of theoretical analysis of the transmitted power of DAB converter, the corresponding switching states of H_1 and H_2 of the full bridge need to be completely replaced according to the change in voltage modulation ratio k. This is not applicable in practical DAB applications, and DPS is proposed [96,97]. In SPS, the internal shift comparison exists in all the primary and secondary sides of the bridge, and the internal shift comparison is the same. Therefore, the AC voltage on both sides of the transformer is a three-level wave. In DPS, D_1 is also defined as the inward shift ratio and D_2 is defined as the outward shift ratio, where $0 \leq D_1 \leq D_2 \leq 1$, and its waveform is shown in Figure 32. Compared with SPS, the backflow power under DPS is relatively reduced, and the converter efficiency is obviously improved. Reference [96] introduced a novel DPS modulation strategy for DAB. In traditional SPS, reactive power is inherent, leading to high peak currents and significant system losses. DPS control eliminates reactive power in isolated bidirectional DC-DC converters. Additionally, compared to traditional SPS, DPS reduces peak inrush and steady-state currents, enhances system efficiency, increases system power capacity, and minimizes the output capacitance. Reference [97] provides a detailed introduction and analysis of DPS and the working principles of the converter. By establishing the mathematical model of transmission power and return power, the control performance of DPS and SPS is compared. Under the same conditions, DPS modulation can effectively reduce the power backflow of the converter, improve the flexibility of power regulation, and thus improve the system efficiency and system power capacity. These properties are especially effective under high voltage conversion ratio and light load conditions.

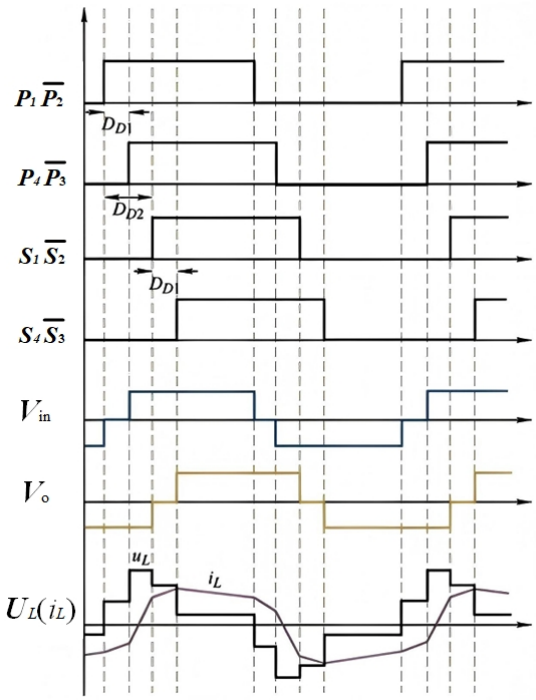

Figure 32. Double-phase shift waveform diagram.

6.4. Triple-Phase Modulation

TPS modulation is proposed in [98] and, similar to DPS modulation, the output AC voltage of both bridges is a three-level wave, and its waveform is shown in Figure 33. The inward shift may not be equal compared to the two sides, so it can control three degrees of free-

dom. TPS modulation consists of an external phase shift angle D_3 and two independently controlled internal phase shift angles D_1 and D_2, located on the primary and secondary sides, respectively. Among the three modulation strategies of SPS, EPS and DPS, it has the greatest potential for performance optimization. SPS modulation, DPS modulation and EPS modulation are special cases of TPS modulation. When $D_1 = D_2 = 1$, TPS modulation can be regarded as SPS modulation. When $D_1 = 1$ or $D_2 = 1$, TPS modulation can be regarded as EPS modulation. When $D_1 = D_2$, TPS modulation can be regarded as DPS modulation. The relationship between the four modulation methods is shown in Figure 34. The DC converter can optimize the modulation parameters more comprehensively on the basis of TPS modulation.

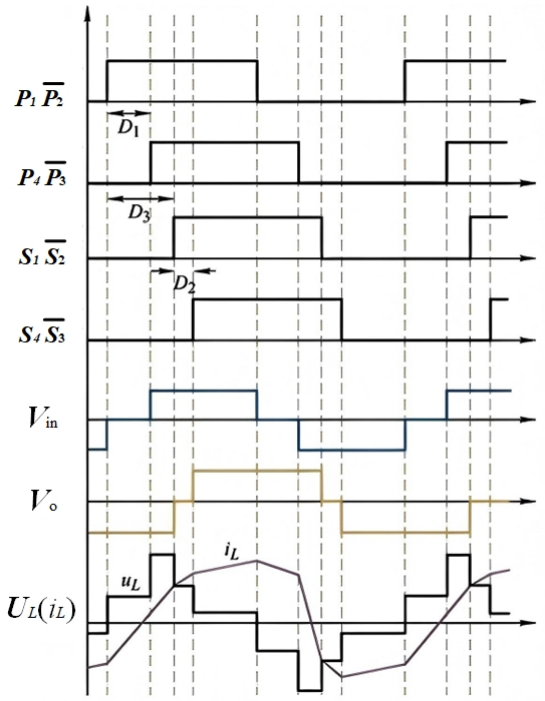

Figure 33. Triple-phase shift waveform diagram.

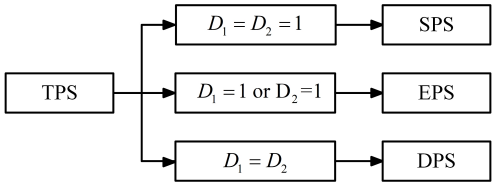

Figure 34. Relationship diagram of four modulation methods.

6.5. Modified Frequency Modulation

In order to reduce converter losses, modified frequency modulation is usually used, combining two or more different modulation techniques to bring their respective advantages into play. The limitation of a single modulation technique is overcome to achieve converter optimization. Modified frequency modulation can automatically switch modulation modes under different load conditions, thereby improving overall efficiency and reducing unnecessary losses. Reference [99] introduces a variable frequency modulation method for a DAB converter, ensuring ZVS with minimal circulating current across a wide power range. The variable frequency modulation algorithm is derived using a generalized power equation. The impact of phase drift is discussed, and a simple compensation scheme is provided to mitigate its effects. Reference [100] proposes a variable frequency modulation scheme that allows DAB converters to operate continuously under full ZVS across the

entire power range, eliminating ZVS losses caused by transitions between modulation regions. This feature extends the ZVS range, thereby improving electromagnetic interference performance and overall power efficiency.

7. Control Strategies

7.1. Proportional Integral Derivative Control

Proportional-integral-derivative (PID) control [101] is a feedback control method used to automatically adjust the system output to maintain it close to the set target value. The algorithm is simple, easy to understand and implement, and is often used in industrial control systems. The control error is generated according to the set and measured output values, and the error is taken as the control parameter of the system according to the relationship between proportional calculation, integral calculation and differential calculation. The control block diagram is shown in Figure 35. However, its performance is highly dependent on parameter adjustment, and for some nonlinear or time-varying systems, the performance is poor, and even the desired control objectives may not be achieved.

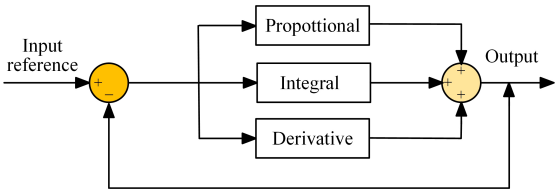

Figure 35. PID control block diagram.

7.2. Sliding Mode Control

Sliding mode control, also known as sliding mode variable structure control, is a control method of variable structure control system, and its overall structure is shown in Figure 36. Since the power electronic converter is a time-varying nonlinear system whose structure changes with the switching device on and off, the sliding mode control is essentially a switching control. By selecting the appropriate switching function and control law, the system state moves on the sliding mode plane, and the output voltage of the converter follows the reference voltage in real time, so as to obtain high precision steady-state output performance, and has good robustness to load changes, input voltage fluctuations and reference voltage fluctuations. Reference [102] proposes a harmonic model for a DAB converter with current feedforward to improve robustness under load variations, but this method requires a large amount of real-time computation. Reference [103] proposed the super-twisting sliding mode control for the DAB converter to enhance the output voltage regulation. The proposed strategy combines the advantages of sliding mode controller and eliminates the tremor problem. The circuit stability is improved by simplifying the design model. Compared with sliding mode control and PID control, the steady-state output voltage ripple is reduced.

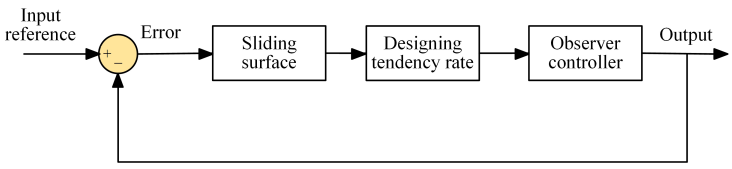

Figure 36. Overall structure of sliding mode controller.

7.3. Fuzzy Control

Fuzzy control method is an intelligent method different from the traditional control method. It does not need to establish a specific mathematical model, but only needs

to summarize the experience and control strategy related to the research object, or find control rules and summarize control rules from a large number of data points, and realize intelligent control of the research object according to these rules. The main function of fuzzy controller is to fuzzy the input variable, convert it into fuzzy signal, and then fuzzy reasoning the fuzzy signal according to fuzzy rules, so as to obtain the output control quantity. In this way, the problems of fuzziness and uncertainty can be transformed into the form of fuzzy rules, which can effectively control the system. The fuzzy controller is composed of fuzzification, knowledge base, fuzzy reasoning and clarity, and its composition structure is shown in Figure 37. It can effectively deal with the inaccuracy of the system, control by empirical rules, does not require accurate mathematical models, and is suitable for complex, non-linear or dynamically changing systems.

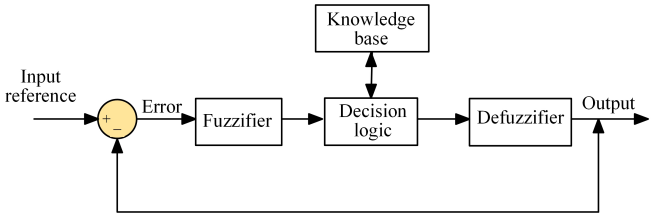

Figure 37. Overall structure of a fuzzy controller.

Reference [104] proposes a fuzzy logic controller scheme for a constant power load DAB converter, which does not require extensive system modeling or prior parameter information. Although it improves performance to some extent, the design process is computationally complex and cumbersome. Stability analysis of fuzzy controllers remains relatively complicated. Fuzzy logic-based controllers are easy to design and implement. Reference [105] presents a fuzzy logic-based energy storage management system using DAB, ensuring a fast dynamic response as the bus voltage and load power demand change, with the charge and discharge voltages adjusting accordingly.

7.4. Boundary Control

Boundary control is a geometric (variable structure) based control method, which is suitable for time-varying nonlinear switching converter circuits. Boundary control has a complete set of large signal analysis tools for the stability and dynamic performance of switching converters. The control idea can be summarized as follows: Based on the large signal trajectory of the state plane of the switching converter, a switching surface is defined to simulate the switching state, and the control algorithm of the switching surface is designed to realize the control of the converter. The state space is divided into two regions by using the designed switching boundary. The switching state is determined by the on-off and on-off motion paths of the converter constantly crossing the switching surface, so as to realize variable structure control. Reference [106] introduces the application of boundary controller in a full-bridge ZVS topology. Under this control scheme, the converter exhibits excellent dynamic performance with no overshoot, optimal response time to startup and load disturbances, and steady-state achieved with a single switching action. In addition to the enhanced dynamic response, steady-state information is used to achieve fixed-frequency operation. Reference [107] introduces a kind of boundary control using DAB converter for constant power load stability. The proposed control is not affected by startup, sudden voltage and power changes, so as to achieve stable operation and fast dynamic response to constant power of the converter. Compared with PID control, the DC bias current is eliminated.

7.5. Model Predictive Control

Model predictive control (MPC), also known as rolling time domain control, models the control system as a discrete time dynamic system and predicts the future state and control signal at each sampling time step. The feedback correction structure is introduced to determine the optimal control signal at the current time, so that the system can achieve the optimal control target in the future. It consists of the following four parts: the prediction model, feedback correction, rolling optimization and reference trajectory; its overall structure is shown in Figure 38.

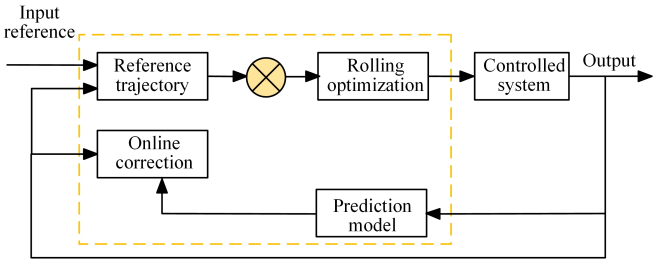

Figure 38. Overall structure of model predictive controller.

Reference [108] proposes a finite control model predictive control for DAB converters in order to achieve faster dynamics and stable operation over the entire power and terminal voltage range, taking into account global control parameters. However, this technology provides flexible multi-target control, and its large signal stability remains problematic. Reference [109] proposed a direct model predictive control for the boost converter, because of the dead zone between the buck and boost conversion, PWM can not achieve the duty ratio. The control operates directly on the switch, completely avoiding the dead zone. Compared to conventional techniques, this technique includes current confinement, avoiding the use of additional current loops.

7.6. Optimization Based on a Meta-Heuristic Algorithm

The meta-heuristic algorithm is iteratively updated in the random search process, and finally a satisfactory approximate solution is obtained. It is a kind of general optimization method, which solves quickly, does not depend on the characteristics of the problem, and only depends on the fitness function value. At present, the genetic algorithm (GA) and particle swarm optimization (PSO) are the most commonly used meta-heuristic methods, which are outstanding in optimizing the efficiency of isolated bidirectional DC-DC converters. These algorithms can solve complex problems effectively and have strong global optimization ability.

7.6.1. Genetic Algorithm

GA is a population search optimization algorithm that does not rely on gradient information, and draws on the genetic and evolutionary mechanism of organisms. It encodes the solution of the problem and operates on this basis, rather than directly encoding the parameters. The genetic algorithm is not only a computational mathematical model of biological evolution, but also a general optimization method to solve optimization problems. Its global search ability and implicit parallel computing ability make it better to solve problems with diversified parameters and high complexity, so it has a wide range of adaptability. In reference [110], genetic algorithm is adopted in the parameter optimization design of the DAB converter to eliminate the problem of high-frequency oscillation and minimize the inductance loss. GA has powerful computational power, which helps to avoid complex theoretical derivation and enables circuit analysis to have a more realistic model.

Literature [111] proposes a multi-objective efficiency optimization scheme based on genetic algorithm and TPS modulation. This method optimizes inductor current stress, inductor root mean square current and ZVS, and reduces on-loss, magnetic loss and switching loss.

7.6.2. PSO Algorithm

The basic aim of the PSO algorithm is to use information sharing among individuals in the group, so the group becomes reasonably ordered in the search space as it moves towards the optimal solution of the problem. It is a global probabilistic search algorithm based on population intelligence, which is derived by simulating the migration and gathering behavior of birds in the process of searching for food. PSO has been widely used in intelligent optimization algorithms because of its advantages such as few parameters, fast operation, strong searching ability and no relation to problem information. In reference [112], the particle swarm optimization strategy was used to optimize three-level modulation phase shift control, and a unified mathematical model of DAB converter based on Fourier transform was constructed to obtain accurate and complex mathematical expressions of inductive current, transmitted power, and reactive power. The proposed method can achieve the minimum reactive power under three-level modulation phase shift control by obtaining the optimal phase shift angle. Literature [113] proposes a minimum current stress scheme based on particle swarm optimization strategy to improve the efficiency of the converter and reduce the current stress. The algorithm adopts two phase shift variables, which not only expands the control flexibility, but also improves the main performance index. In addition to this, the PSO strategy has fewer parameters to adjust, less computational burden, faster convergence, and simplifies theoretical calculation and practical implementation.

7.7. Artificial Intelligence Control

The application of artificial intelligence (AI) in the PV DC converter uses the self-learning and self-adaptive ability of neural network to build a neural network model. Learn the output characteristics of PV cells under different light intensity, temperature and other conditions, so as to accurately find the maximum power point. The neural network is trained by a large amount of sample data to learn the mapping relationship between input and output, so as to adjust the operating point of the bidirectional DC converter in real time, so that it always runs near the maximum power point, and improve the efficiency of PSG. Neural network control methods implement activities that mimic and replicate human neural networks, enabling converters to adjust and enhance performance in real time. In order to maintain optimal performance, the neural network control method continuously monitors the input and desired output of the converter and adjusts the corresponding control signal in time. The control can handle complex nonlinear relationships, has good dynamic performance and adaptability, and performs well in dealing with complex working conditions and load changes. By using the AI algorithm to monitor and analyze the operation data of PV DC converter in real time, early signs of failure can be found in time. This improves system reliability and safety, reducing downtime and maintenance costs. In addition to this, the AI control can dynamically adjust the working mode and parameters of the PV DC converter according to the real-time operation data to improve the overall efficiency of the system.

Reference [114] proposes a hybrid model based on an artificial neural network maximum power point-tracking algorithm. This strategy uses a photovoltaic cell model with a multi-layer perceptron structure to approximate the short circuit current through this and uses it as auxiliary information of PSO algorithm to achieve fast and accurate tracking performance. Reference [115] analyzes control methods based on adaptive neural fuzzy inference systems (ANFIS), PI controllers optimized using PSO and GA, and explores

the performance of artificial neural network (ANN) controls. The results show that both ANFIS controller and PI controller optimized by PSO and GA can achieve accurate output voltage regulation. When the input voltage is fixed, the ANN control method outperforms other methods, showing excellent performance in terms of rise time, transient time, stable time, and peak time. On the contrary, under different input voltage conditions, the ANFIS control method shows excellent performance in terms of transient time and peak time. Reference [116] proposes a DC-DC switching converter controller based on the AI algorithm, which is simpler in structure than the traditional neural network-PID controller. It can realize modelless control, has strong adaptive ability, and can be applied to different kinds of DC-DC converters. As a result, the proposed controller has excellent transient response performance. Compared with other controllers, the transient performance is significantly improved. The advantages and disadvantages of various control techniques are shown in Table 4.

Table 4. Advantages and disadvantages of various control technologies.

References	Control Strategy	Advantages	Disadvantages
[101]	PID	The algorithm is simple, robust and reliable	Lack of adaptive ability
[102,103]	Sliding mode control	Better convergence and transient response	Modeling is relatively complex
[104,105]	Fuzzy control	Accurate mathematical models are not required, good handling of nonlinearity	High requirements for sampling frequency
[106,107]	Boundary control	Global stability of the system; good working characteristics of large signals; fast dynamic response	The complexity and instability of multi boundary condition combinations
[108,109]	Model predictive control	Effectively combating environmental uncertainty and time delay	Computational complexity depends on the accuracy of the model
[110–113]	Optimization based on a meta-heuristic algorithm	Self-learning function; Strong adaptability	Low response speed; susceptible to parameters
[114–116]	Artificial intelligence control	Improve efficiency strong stability optimize control strategy	Data dependence is strong model training is complex and time-consuming and professional and technical requirements are high

8. Conclusions

This paper conducts an in-depth study of bidirectional DC-DC converters in PGS. With the growing concerns over the greenhouse effect and environmental pollution, there is an urgent need to develop renewable energy sources. Due to its ease of installation and low operational costs, PGS has become a highly regarded technological option. In PGS, efficient and high-power-density bidirectional DC-DC converters are essential. These converters are implemented by replacing unidirectional switches or by adding a transformer to achieve electrical isolation, forming a bidirectional isolated DC-DC converter topology. The basic principles of bidirectional DC-DC converters are explained in detail, along with an analysis of their characteristics, efficiency, complexity, and application scenarios. Current research primarily focuses on reducing weight, size, losses, and costs while improving reliability and power density. Additionally, the principles of switching strategies and control schemes are explored, comparing the advantages and disadvantages of different control strategies to help select the most suitable one for specific applications. This aims to reduce circulating current, current stress, and conduction losses, while expanding the ZVS operating range. Ultimately, the goal is to design a highly reliable and efficient soft-switching control strategy.

On the hardware side, efforts are made to reduce additional components and variable frequencies to achieve ZVS or ZCS for all switches in all modes.

Author Contributions: Conceptualization: A.T.; Data curation: Z.X.; Funding acquisition: A.T.; Software: Z.X., Q.C. and T.S.; Resources: A.T.; Writing—original draft: Z.X.; Writing—review and editing: A.T. All authors have read and agreed to the published version of the manuscript.

Funding: This research was funded by the Tianchi Talent Program of Xinjiang Uygur Autonomous, Basic Scientific Research Project Funded by the General Research and Development Expenditure of Universities in the Xinjiang Uygur Autonomous Region, grant number XJEDU2023P027, Science and Technology Project of Xinjiang Uygur Autonomous Region—Major Science and Technology Project, grant number 2022A01007-4, Research on Integrated Energy System of Hydrogen Energy Storage Coupled with Coal Chemical Industry in Xinjiang, grant number 52266018 and Research on the Integrated Energy System with Multiple Types of Energy Storage for Advanced Power Systems with the "Source-Grid-Load-Storage" Integration Approach, grant number 2022TSYCCX0051.

Acknowledgments: We sincerely appreciate the thoughtful opinions and invaluable suggestions provided by the anonymous reviewers.

Conflicts of Interest: The authors declare no conflicts of interest.

References

1. Paraschiv, L.S.; Paraschiv, S. Contribution of renewable energy (hydro, wind, solar and biomass) to decarbonization and transformation of the electricity generation sector for sustainable development. *Energy Rep.* **2023**, *9*, 535–544. [CrossRef]
2. Poti, K.D.; Naidoo, R.M.; Mbungu, N.T.; Bansal, R.C. Intelligent solar photovoltaic power forecasting. *Energy Rep.* **2023**, *9*, 343–352. [CrossRef]
3. Wai, R.-J.; Wang, W.-H. Grid-connected photovoltaic generation system. *IEEE Trans. Circuits Syst. I Regul. Pap.* **2008**, *55*, 953–964.
4. Lal, V.N.; Singh, S.N. Control and performance analysis of a single-stage utility-scale grid-connected pv system. *IEEE Syst. J.* **2017**, *11*, 1601–1611. [CrossRef]
5. Zhu, X.; Hu, H.; Tao, H.; He, Z. Stability analysis of pv plant-tied mvdc railway electrification system. *IEEE Trans. Transp.* **2019**, *5*, 311–323. [CrossRef]
6. Alkhaldi, A.; Elkhateb, A.; Laverty, D. Voltage lifting techniques for non-isolated dc/dc converters. *Electronics* **2023**, *12*, 718. [CrossRef]
7. Kanaparthi, R.K.; Singh, J.P.; Ballal, M.S. A review on multi-port bidirectional isolated and non-isolated dc-dc converters for renewable applications. In Proceedings of the 2022 IEEE International Conference on Power Electronics, Drives and Energy Systems (PEDES), Jaipur, India, 14–17 December 2022; pp. 1–6.
8. Costa, L.F.; Buticchi, G.; Liserre, M. Optimum design of a multiple-active-bridge dc–dc converter for smart transformer. *IEEE Trans. Power Electron.* **2018**, *33*, 10112–10121. [CrossRef]
9. Li, Y.; Wang, R.; Zhong, L.; Mao, L.; Sun, C.; Li, X.; Hu, S. Analysis and design of a high-frequency isolated dual-transformer dc-dc resonant converter. *Electronics* **2022**, *12*, 103. [CrossRef]
10. Zhang, H.; Wang, S.; Li, Y.; Wang, Q.; Fu, D. Two-capacitor transformer winding capacitance models for common-mode emi noise analysis in isolated dc–dc converters. *IEEE Trans. Power Electron.* **2017**, *32*, 8458–8469. [CrossRef]
11. Ortíz-Marín, J.; Gallo-Reyes, D.; Ruiz-Robles, D.; Venegas-Rebollar, V. Analyzing power losses and performance of an isolated dc-dc converter for renewable energies systems. *Electronics* **2023**, *12*, 1110. [CrossRef]
12. Venkatramanan, D.; John, V. Dynamic modeling and analysis of buck converter based solar pv charge controller for improved mppt performance. *IEEE Trans. Ind. Appl.* **2019**, *55*, 6234–6246. [CrossRef]
13. Forouzesh, M.; Siwakoti, Y.P.; Gorji, S.A.; Blaabjerg, F.; Lehman, B. Step-up dc–dc converters: A comprehensive review of voltage-boosting techniques, topologies, and applications. *IEEE Trans. Power Electron.* **2017**, *32*, 9143–9178. [CrossRef]
14. Alavi, P.; Babaei, E.; Mohseni, P.; Marzang, V. Study and analysis of a dc–dc soft-switched buck converter. *IET Power Electron.* **2020**, *13*, 1456–1465. [CrossRef]
15. Talebian, I.; Alavi, P.; Marzang, V.; Babaei, E.; Khoshkbar-Sadigh, A. Analysis, design, and investigation of a soft-switched buck converter with high efficiency. *IEEE Trans. Power Electron.* **2022**, *37*, 6899–6912. [CrossRef]
16. Hu, X.; Gong, C. A high voltage gain dc–dc converter integrating coupled-inductor and diode–capacitor techniques. *IEEE Trans. Power Electron.* **2014**, *29*, 789–800.
17. Rezvanyvardom, M.; Mirzaei, A. Zero-voltage transition nonisolated bidirectional buck–boost dc–dc converter with coupled inductors. *IEEE J. Emerg. Sel. Top. Power Electron.* **2021**, *9*, 3266–3275. [CrossRef]

18. Gholizadeh, H.; Gorji, S.A.; Sera, D. A quadratic buck-boost converter with continuous input and output currents. *IEEE Access* **2023**, *11*, 22376–22393. [CrossRef]
19. Zhou, Y.; Li, J.; Liu, X.; Zheng, Y.; Leung, K.N. Bidirectional buck–boost converter with reduced power loss and no right-half-plane zero. *IEEE Trans. Power Electron.* **2023**, *38*, 2127–2142. [CrossRef]
20. Veerachary, M. Bi-polar buck-boost converter. *IEEE Trans. Circuits Syst. II Express Briefs* **2024**, 71, 2429–2433. [CrossRef]
21. Mo, L.; Wang, Y.; Jiang, C.; Wang, X.; Zhang, B. A novel topology derivation method revealed from classical cuk, sepic, and zeta converters. *IEEE Trans. Power Electron.* **2024**, *39*, 7828–7833. [CrossRef]
22. Almalaq, Y.; Matin, M. Three topologies of a non-isolated high gain switched-inductor switched-capacitor step-up cuk converter for renewable energy applications. *Electronics* **2018**, *7*, 94. [CrossRef]
23. Song, M.-S.; Son, Y.-D.; Lee, K.-H. Non-isolated bidirectional soft-switching sepic/zeta converter with reduced ripple currents. *J. Power Electron.* **2014**, *14*, 649–660. [CrossRef]
24. Kim, I.-D.; Paeng, S.-H.; Ahn, J.-W.; Nho, E.-C.; Ko, J.-S. New bidirectional zvs pwm sepic/zeta dc-dc converter. In Proceedings of the 2007 IEEE International Symposium on Industrial Electronics, Vigo, Spain, 4–7 June 2007; pp. 555–560.
25. Ardi, H.; Ajami, A. Study on a high voltage gain sepic-based dc–dc converter with continuous input current for sustainable energy applications. *IEEE Trans. Power Electron.* **2018**, *33*, 10403–10409. [CrossRef]
26. Ghojavand, H.; Adib, E. A single-switch soft-switched high step-down zeta converter with low output current ripple. *IEEE Trans. Power Electron.* **2023**, *38*, 5024–5031. [CrossRef]
27. Kamalinejad, K.; Iman-Eini, H.; Aleyasin, S.H.; Ghadi, M.A. A novel nonisolated buck–boost dc–dc converter with low voltage stress on components. *IEEE J. Emerg. Sel. Top. Ind. Electron.* **2023**, *4*, 492–501. [CrossRef]
28. Sadeghpour, D.; Bauman, J. A generalized method for comprehension of switched-capacitor high step-up converters including coupled inductors and voltage multiplier cells. *IEEE Trans. Power Electron.* **2021**, *37*, 5801–5815. [CrossRef]
29. Qian, W.; Cao, D.; Cintron-Rivera, J.G.; Gebben, M.; Wey, D.; Peng, F.Z. A switched-capacitor dc–dc converter with high voltage gain and reduced component rating and count. *IEEE Trans. Ind. Appl.* **2012**, *48*, 1397–1406. [CrossRef]
30. Cockcroft, J.D.; Walton, E.T. Experiments with high velocity positive ions.—(i) further developments in the method of obtaining high velocity positive ions. *Proc. R. Soc. Lond. Ser. A Contain. Pap. Math. Phys. Character* **1932**, *136*, 619–630.
31. Kumar, G.G.; Sundaramoorthy, K.; Karthikeyan, V.; Babaei, E. Switched capacitor–inductor network based ultra-gain dc–dc converter using single switch. *IEEE Trans. Ind. Electron.* **2020**, *67*, 10274–10283. [CrossRef]
32. Xie, H.; Li, R. A novel switched-capacitor converter with high voltage gain. *IEEE Access* **2019**, *7*, 107831–107844. [CrossRef]
33. Sadaf, S.; Bhaskar, M.S.; Meraj, M.; Iqbal, A.; Al-Emadi, N. A novel modified switched inductor boost converter with reduced switch voltage stress. *IEEE Trans. Ind. Electron.* **2020**, *68*, 1275–1289. [CrossRef]
34. Bao, D.; Kumar, A.; Pan, X.; Xiong, X.; Beig, A.R.; Singh, S.K. Switched inductor double switch high gain dc-dc converter for renewable applications. *IEEE Access* **2021**, *9*, 14259–14270. [CrossRef]
35. Pirpoor, S.; Rahimpour, S.; Andi, M.; Kanagaraj, N.; Pirouzi, S.; Mohammed, A.H. A novel and high-gain switched-capacitor and switched-inductor-based dc/dc boost converter with low input current ripple and mitigated voltage stresses. *IEEE Access* **2022**, *10*, 32782–32802. [CrossRef]
36. Faridpak, B.; Bayat, M.; Nasiri, M.; Samanbakhsh, R.; Farrokhifar, M. Improved hybrid switched inductor/switched capacitor dc–dc converters. *IEEE Trans. Power Electron.* **2020**, *36*, 3053–3062. [CrossRef]
37. Luo, P.; Liang, T.-J.; Chen, K.-H.; Chen, S.-M. Design and implementation of a high step-up dc-dc converter with active switched inductor and coupled inductor. *IEEE Trans. Ind. Appl.* **2023**, *59*, 3470–3480. [CrossRef]
38. Mizani, A.; Ansari, S.A.; Shoulaie, A.; Davidson, J.N.; Foster, M.P. Single-active switch high-voltage gain dc–dc converter using a non-coupled inductor. *IET Power Electron.* **2021**, *14*, 492–502. [CrossRef]
39. Chen, S.; Zhou, L.; Luo, Q.; Gao, W.; Wei, Y.; Sun, P.; Du, X. Research on topology of the high step-up boost converter with coupled inductor. *IEEE Trans. Power Electron.* **2019**, *34*, 10733–10745. [CrossRef]
40. Harasimczuk, M.; Kopacz, R.; Tomaszuk, A. Lossless clamp circuit with turn-off voltage and current reduction in high step-up dc/dc converter with coupled inductor. *IEEE Trans. Power Electron.* **2023**, *39*, 1074–1086. [CrossRef]
41. Rao, B.T.; De, D. Effective leakage energy recycling in high gain dc-dc converter with coupled inductor. *IEEE Trans. Circuits Syst. II Express Briefs* **2022**, *69*, 3284–3288.
42. Kumar, M.; Gupta, J.K.; Verma, A.K.; Sandeep, N. Coupled inductor based soft-switched ultra high-gain converter with voltage quadrupler cell. In Proceedings of the 2022 IEEE Global Conference on Computing, Power and Communication Technologies (GlobConPT), New Delhi, India, 23–25 September 2022; IEEE: Piscataway, NJ, USA, 2022; pp. 1–7.
43. Wu, T.-F.; Yu, T.-H. Unified approach to developing single-stage power converters. *IEEE Trans. Aerosp. Electron. Syst.* **1998**, *34*, 211–223.
44. Nikbakht, M.; Abbasian, S.; Farsijani, M.; Abbaszadeh, K. An ultra high gain double switch quadratic boost coupled inductor based converter. In Proceedings of the 2022 13th Power Electronics, Drive Systems, and Technologies Conference (PEDSTC), Tehran, Iran, 1–3 February 2022; IEEE: Piscataway, NJ, USA, 2022; pp. 167–172.

45. Zhang, H.; Park, S.-J. Efficiency optimization method for cascaded two-stage boost converter. *IEEE Access* **2022**, *10*, 53443–53453. [CrossRef]
46. Vighetti, S.; Ferrieux, J.-P.; Lembeye, Y. Optimization and design of a cascaded dc/dc converter devoted to grid-connected photovoltaic systems. *IEEE Trans. Power Electron.* **2012**, *27*, 2018–2027. [CrossRef]
47. Parizi, M.K.B.; Emamjomeh, S.S.; Khorasani, R.R.; Behzadnezhad, M.A.; Adib, E.; Kavehvash, Z. Design and implementation of an interleaved high efficiency and high voltage gain converter with minimum switch count for renewable energy integration. *IEEE Trans. Ind.* **2024**, *71*, 5863–5870. [CrossRef]
48. Kothapalli, K.R.; Ramteke, M.R.; Suryawanshi, H.M.; Reddi, N.K.; Kalahasthi, R.B. Soft-switched ultrahigh gain dc–dc converter with voltage multiplier cell for dc microgrid. *IEEE Trans. Ind. Electron.* **2021**, *68*, 11063–11075. [CrossRef]
49. Singh, K.A.; Prajapati, A.; Chaudhary, K. High-gain compact interleaved boost converter with reduced voltage stress for pv application. *IEEE J. Emerg. Sel. Top. Power Electron.* **2021**, *10*, 4763–4770. [CrossRef]
50. Alghaythi, M.L.; O'Connell, R.M.; Islam, N.E.; Khan, M.M.S.; Guerrero, J.M. A high step-up interleaved dc-dc converter with voltage multiplier and coupled inductors for renewable energy systems. *IEEE Access* **2020**, *8*, 123165–123174. [CrossRef]
51. Zhang, X.; Green, T.C. The modular multilevel converter for high step-up ratio dc–dc conversion. *IEEE Trans. Ind. Electron.* **2015**, *62*, 4925–4936. [CrossRef]
52. Kung, S.H.; Kish, G.J. A modular multilevel hvdc buck–boost converter derived from its switched-mode counterpart. *IEEE Trans. Power Deliv.* **2017**, *33*, 82–92. [CrossRef]
53. Gray, P.A.; Lehn, P.W.; Yakop, N. A modular multilevel dc–dc converter with flying capacitor converter like properties. *IEEE Trans. Ind. Electron.* **2021**, *69*, 6774–6783. [CrossRef]
54. Samanbakhsh, R.; Ibanez, F.M.; Koohi, P.; Martin, F. A new asymmetric cascaded multilevel converter topology with reduced voltage stress and number of switches. *IEEE Access* **2021**, *9*, 92276–92287. [CrossRef]
55. Li, M.; Ouyang, Z.; Andersen, M.A. Analysis and optimal design of high-frequency and high-efficiency asymmetrical half-bridge flyback converters. *IEEE Trans. Ind. Electron.* **2019**, *67*, 8312–8321. [CrossRef]
56. Zhang, J.; Huang, X.; Wu, X.; Qian, Z. A high efficiency flyback converter with new active clamp technique. *IEEE Trans. Power Electron.* **2010**, *25*, 1775–1785. [CrossRef]
57. Konar, S.; Saha, S.S. Efficient energy recovery and boosting the voltage gain of a soft-switched flyback converter. In Proceedings of the 2020 IEEE International Conference on Power Electronics, Drives and Energy Systems (PEDES), Jaipur, India, 16–19 December 2020; IEEE: Piscataway, NJ, USA, 2020; pp. 1–5.
58. Lagap, T.; Dimopoulos, E.; Munk-Nielsen, S. An rcdd snubber for a bidirectional flyback converter. In Proceedings of the 2015 17th European Conference on Power Electronics and Applications (EPE'15 ECCE-Europe), Geneva, Switzerland, 8–10 September 2015; pp. 1–10.
59. Park, H.-P.; Jung, J.-H. Design methodology of quasi-resonant flyback converter with a divided resonant capacitor. *IEEE Trans. Ind. Electron.* **2020**, *68*, 10796–10805. [CrossRef]
60. Hsieh, Y.-C.; Chen, M.-R.; Cheng, H.-L. An interleaved flyback converter featured with zero-voltage transition. *IEEE Trans. Power Electron.* **2010**, *26*, 79–84. [CrossRef]
61. Tonolo, É.A.; Soares, J.W.M.; Badin, A.A.; Alonso, J.M. Frequency-modulated high-gain boost–flyback dc–dc converter for renewable energy systems. *IEEE Trans. Ind. Electron.* **2023**, *71*, 10772–10782. [CrossRef]
62. Allahyari, H.; Latifzadeh, M.A.; Bahrami, H.; Adib, E.; Faezi, H. An improved single switch wide range zvs forward converter controlled with variable magnetizing inductance. *IEEE J. Emerg. Sel. Top. Ind. Electron.* **2023**, *5*, 837–847. [CrossRef]
63. Jang, P.; Cho, B.-H. Two-switch forward converter with reset winding and an auxiliary active-clamp circuit for a wide input voltage range. *IEEE Trans. Power Electron.* **2016**, *32*, 4491–4502. [CrossRef]
64. Wuti, V.; Trakuldit, S.; Luangpol, A.; Tattiwong, K.; Taylim, A.; Bunlaksananusorn, C. A simplified analysis and design of an rcd clamp forward converter. In Proceedings of the 2022 8th International Conference on Engineering, Applied Sciences, and Technology (ICEAST), Chiang Mai, Thailand, 8–10 June 2022; IEEE: Piscataway, NJ, USA, 2022; pp. 97–100.
65. Lakshmi, G. A dual-transformer active-clamp forward converter using a single switch. In Proceedings of the 2017 International Conference on Computation of Power, Energy Information and Commuincation (ICCPEIC), Melmaruvathur, India, 22–23 March 2017; IEEE: Piscataway, NJ, USA, 2017; pp. 660–663.
66. Jeong, Y.; Park, J.-D.; Moon, G.-W. An interleaved active-clamp forward converter modified for reduced primary conduction loss without additional components. *IEEE Trans. Power Electron.* **2019**, *35*, 121–130. [CrossRef]
67. Murakami, N.; Yamasaki, M. Analysis of a resonant reset condition for a single-ended forward converter. In Proceedings of the PESC' 88 Record: 19th Annual IEEE Power Electronics Specialists Conference, Kyoto, Japan, 11–14 April 1988; pp. 1018–1023.
68. Lim, J.-W.; Hassan, J.; Kim, M. Bidirectional soft switching push–pull resonant converter over wide range of battery voltages. *IEEE Trans. Power Electron.* **2021**, *36*, 12251–12267. [CrossRef]
69. Wang, C.; Li, M.; Ouyang, Z.; Wang, G. Resonant push–pull converter with flyback regulator for mhz high step-up power conversion. *IEEE Trans. Ind. Electron.* **2021**, *68*, 1178–1187. [CrossRef]

70. Jiang, L.; Wan, J.; Li, Y.; Huang, C.; Liu, F.; Wang, H.; Sun, Y.; Cao, Y. A new push-pull dc/dc converter topology with complementary active clamped. *IEEE Trans. Ind. Electron.* **2022**, *69*, 6445–6449. [CrossRef]
71. Nayanasiri, D.R.; Foo, G.H.B.; Vilathgamuwa, D.M.; Maskell, D.L. A switching control strategy for single- and dual-inductor current-fed push–pull converters. *IEEE Trans. Power Electron.* **2015**, *30*, 3761–3771. [CrossRef]
72. Shi, H.; Sun, K.; Wu, H.; Li, Y. A unified state-space modeling method for a phase-shift controlled bidirectional dual-active half-bridge converter. *IEEE Trans. Power Electron.* **2019**, *35*, 3254–3265. [CrossRef]
73. Meghdad, T.; Jafar, M.; Bijan, A. High step-up current-fed zvs dual half-bridge dc–dc converter for high-voltage applications. *IET Power Electron.* **2015**, *8*, 309–318. [CrossRef]
74. Yeon, C.-O.; Lee, J.-B.; Lee, I.-O.; Moon, G.-W. Wide zvs range asymmetric half-bridge converter with clamp switch and diode for high conversion efficiency. *IEEE Trans. Ind. Electron.* **2016**, *63*, 2862–2870. [CrossRef]
75. Leu, C.-S.; Nha, Q.T. A half-bridge converter with input current ripple reduction for dc distribution systems. *IEEE Trans. Power Electron.* **2013**, *28*, 1756–1763. [CrossRef]
76. Chakraborty, S.; Chattopadhyay, S. Minimum-rms-current operation of asymmetric dual active half-bridge converters with and without zvs. *IEEE Trans. Power Electron.* **2017**, *32*, 5132–5145. [CrossRef]
77. Beibei, R.; Dan, W.; Chengxiong, M.; Jun, Q.; Jiangang, Z. Analysis of full bridge dc-dc converter in power system. In Proceedings of the 2011 4th International Conference on Electric Utility Deregulation and Restructuring and Power Technologies (DRPT), Weihai, China, 6–9 July 2011; pp. 1242–1245.
78. Wang, H.; Sun, Q.; Chung, H.S.H.; Tapuchi, S.; Ioinovici, A. A zcs current-fed full-bridge pwm converter with self-adaptable soft-switching snubber energy. *IEEE Trans. Power Electron.* **2009**, *24*, 1977–1991. [CrossRef]
79. Lo, Y.-K.; Lin, C.-Y.; Hsieh, M.-T.; Lin, C.-Y. Phase-shifted full-bridge series-resonant dc-dc converters for wide load variations. *IEEE Trans. Ind. Electron.* **2011**, *58*, 2572–2575. [CrossRef]
80. Lee, J.-P.; Min, B.-D.; Kim, T.-J.; Yoo, D.-W.; Yoo, J.-Y. A novel topology for photovoltaic dc/dc full-bridge converter with flat efficiency under wide pv module voltage and load range. *IEEE Trans. Ind. Electron.* **2008**, *55*, 2655–2663. [CrossRef]
81. Nguyen, T.-T.; Cha, H.; Kim, H.-G. Current-fed quasi-z-source full-bridge isolated dc–dc converter. *IEEE Trans. Ind. Electron.* **2021**, *68*, 12046–12057. [CrossRef]
82. Wei, Y.; Luo, Q.; Mantooth, H.A. A resonant frequency tracking technique for llc converter-based dc transformers. *IEEE J. Emerg. Selected Top. Ind. Electron.* **2021**, *2*, 579–590. [CrossRef]
83. Hou, N.; Gunawardena, P.; Wu, X.; Ding, L.; Zhang, Y.; Li, Y.W. An input-oriented power sharing control scheme with fast-dynamic response for isop dab dc–dc converter. *IEEE Trans. Power Electron.* **2021**, *37*, 6501–6510. [CrossRef]
84. Min, J.; Ordonez, M. Bidirectional resonant cllc charger for wide battery voltage range: Asymmetric parameters methodology. *IEEE Trans. Power Electron.* **2020**, *36*, 6662–6673. [CrossRef]
85. Zhou, J.; Ma, H. A new llc converter with wide output voltage range and improved efficiency at medium or low output voltage. In Proceedings of the 2019 IEEE 28th International Symposium on Industrial Electronics (ISIE), Vancouver, BC, Canada, 12–14 June 2019; pp. 734–739.
86. Wang, H.; Cheng, C.; Xie, S. Study on a modified cllc converter paralleling a resonant branch with the transformer for wide voltage range applications. *IEEE Access* **2024**, *12*, 32788–32800. [CrossRef]
87. Shen, Y.; Wang, H.; Al-Durra, A.; Qin, Z.; Blaabjerg, F. A structure-reconfigurable series resonant dc–dc converter with wide-input and configurable-output voltages. *IEEE Trans. Ind. Appl.* **2019**, *55*, 1752–1764. [CrossRef]
88. Jia, P.; Su, Z.; Shao, T.; Mei, Y. An isolated high step-up converter based on the active secondary-side quasi-resonant loops. *IEEE Trans. Power Electron.* **2022**, *37*, 659–673. [CrossRef]
89. Kanagaraj, N.; Ramasamy, M.; Vijayakumar, M.; Aldosari, O. Design of an extendable high boost multi-port z-network converter for small power grid-connected pv applications. *IEEE Open J. Power Electron.* **2024**, *5*, 534–553.
90. Qian, T.; Yang, Y.; Zhao, W. A boost-type three-port resonant forward converter with flexible power flow path optimization for pv systems. *IEEE Trans. Circuits Syst. II Express Briefs* **2023**, *70*, 161–165. [CrossRef]
91. Zeng, J.; Qiao, W.; Qu, L. An isolated three-port bidirectional dc–dc converter for photovoltaic systems with energy storage. *IEEE Trans. Ind. Appl.* **2015**, *51*, 3493–3503. [CrossRef]
92. Sun, X.; Shen, Y.; Li, W.; Wu, H. A pwm and pfm hybrid modulated three-port converter for a standalone pv/battery power system. *IEEE J. Emerg. Sel. Top. Power Electron.* **2015**, *3*, 984–1000. [CrossRef]
93. Chen, X.; Xu, G.; Han, H.; Liu, D.; Sun, Y.; Su, M. Light-load efficiency enhancement of high-frequency dual-active-bridge converter under sps control. *IEEE Trans. Ind. Electron.* **2021**, *68*, 12941–12946. [CrossRef]
94. Chen, X.; Xu, J.; Xu, G. Hybrid sps control for isop dual-active-bridge converter based on modulated coupled inductor with full load range zvs and rms current optimization in dc transformer applications. *IEEE Access* **2022**, *10*, 131394–131405. [CrossRef]
95. Zhao, B.; Yu, Q.; Sun, W. Extended-phase-shift control of isolated bidirectional dc–dc converter for power distribution in microgrid. *IEEE Trans. Power Electron.* **2012**, *27*, 4667–4680. [CrossRef]

96. Bai, H.; Mi, C. Eliminate reactive power and increase system efficiency of isolated bidirectional dual-active-bridge dc–dc converters using novel dual-phase-shift control. *IEEE Trans. Power Electron.* **2008**, *23*, 2905–2914. [CrossRef]
97. Zhao, B.; Song, Q.; Liu, W.; Sun, W. Current-stress-optimized switching strategy of isolated bidirectional dc–dc converter with dual-phase-shift control. *IEEE Trans. Ind. Electron.* **2013**, *60*, 4458–4467. [CrossRef]
98. Krismer, F.; Kolar, J.W. Accurate small-signal model for the digital control of an automotive bidirectional dual active bridge. *IEEE Trans. Power Electron.* **2009**, *24*, 2756–2768. [CrossRef]
99. Hiltunen, J.; Väisänen, V.; Juntunen, R.; Silventoinen, P. Variable-frequency phase shift modulation of a dual active bridge converter. *IEEE Trans. Power Electron.* **2015**, *30*, 7138–7148. [CrossRef]
100. Lyu, D.; Straathof, C.; Soeiro, T.B.; Qin, Z.; Bauer, P. Zvs-optimized constant and variable switching frequency modulation schemes for dual active bridge converters. *IEEE Open J. Power Electron.* **2023**, *4*, 801–816. [CrossRef]
101. Arya, S.R.; Maurya, R.; Naidu, T.A.; Babu, B.C. Adaptive observer for dynamic voltage restorer with optimized proportional integral gains. *Chin. J. Electr. Eng.* **2022**, *8*, 38–52. [CrossRef]
102. Segaran, D.; Holmes, D.G.; McGrath, B.P. Enhanced load step response for a bidirectional dc–dc converter. *IEEE Trans. Power Electron.* **2013**, *28*, 371–379. [CrossRef]
103. Tiwary, N.; Panda, V.N.N.A.K.; Narendra, A.; Lenka, R.K. A robust voltage control of dab converter with super-twisting sliding mode approach. *IEEE J. Emerg. Sel. Top. Ind. Electron.* **2023**, *4*, 288–298. [CrossRef]
104. Liu, B.; Zha, Y.; Zhang, T.; Chen, S. Fuzzy logic control of dual active bridge in solid state transformer applications. In Proceedings of the 2016 Tsinghua University-IET Electrical Engineering Academic Forum, Beijing, China, 13–15 May 2016; pp. 1–4.
105. Khan, M.M.S.; Faruque, M.O.; Newaz, A. Fuzzy logic based energy storage management system for mvdc power system of all electric ship. *IEEE Trans. Energy Convers.* **2017**, *32*, 798–809. [CrossRef]
106. Oggier, G.G.; Ordonez, M. Boundary control of full-bridge zvs: Natural switching surface for transient and steady-state operation. *IEEE Trans. Ind. Electron.* **2014**, *61*, 969–979. [CrossRef]
107. Cao, Z.; Wen, H.; Bu, Q.; Shi, H.; Xu, P.; Yang, Y.; Du, Y. Constant power load stabilization with fast transient boundary control for dab-converters-based electric drive systems. *IEEE Trans. Ind. Electron.* **2024**, *71*, 1863–1874. [CrossRef]
108. Tarisciotti, L.; Chen, L.; Shao, S.; Dragičević, T.; Wheeler, P.; Zanchetta, P. Finite control set model predictive control for dual active bridge converter. *IEEE Trans. Ind. Appl.* **2021**, *58*, 2155–2165. [CrossRef]
109. Ullah, B.; Ullah, H.; Khalid, S. Direct model predictive control of noninverting buck-boost dc-dc converter. *CES Trans. Electr. Mach. Syst.* **2022**, *6*, 332–339. [CrossRef]
110. Wang, C.; Zsurzsan, T.-G.; Zhang, Z. Genetic algorithm assisted parametric design of splitting inductance in high frequency gan-based dual active bridge converter. *IEEE Trans. Ind. Electron.* **2023**, *70*, 522–531. [CrossRef]
111. Zhou, L.; Gao, Y.; Ma, H.; Krein, P.T. Wide-load range multiobjective efficiency optimization produces closed-form control solutions for dual active bridge converter. *IEEE Trans. Power Electron.* **2021**, *36*, 8612–8616. [CrossRef]
112. Shi, H.; Wen, H.; Hu, Y.; Jiang, L. Reactive power minimization in bidirectional dc–dc converters using a unified-phasor-based particle swarm optimization. *IEEE Trans. Power Electron.* **2018**, *33*, 10990–11006. [CrossRef]
113. Wang, Y.; Wen, H.; Zhu, Y.; Shi, H.; Bu, Q.; Hu, Y.; Yang, Y. Minimum-current-stress scheme of three-level dual-active-bridge dc–dc converters with the particle swarm optimization. *IEEE Trans. Transp. Electrif.* **2021**, *7*, 2067–2084. [CrossRef]
114. Khosravi, M.; Heshmatian, S.; Khaburi, D.A.; Garcia, C.; Rodriguez, J. A novel hybrid model-based mppt algorithm based on artificial neural networks for photovoltaic applications. In Proceedings of the 2017 IEEE Southern Power Electronics Conference (SPEC), Puerto Varas, Chile, 4–7 December 2017; IEEE: Piscataway, NJ, USA, 2017; pp. 1–6.
115. Saha, U.; Shahria, S.; Rashid, A.H.-U. Intelligent control strategies for dc-dc boost converter: Performance analysis and optimization. In Proceedings of the 2023 International Conference on Smart Systems for Applications in Electrical Sciences (ICSSES), Tumakuru, India, 7–8 July 2023; IEEE: Piscataway, NJ, USA, 2023; pp. 1–6.
116. Shi, X.; Chen, N.; Wei, T.; Wu, J.; Xiao, P. A reinforcement learning-based online-training ai controller for dc-dc switching converters. In Proceedings of the 2021 6th International Conference on Integrated Circuits and Microsystems (ICICM), Nanjing, China, 22–24 October 2021; IEEE: Piscataway, NJ, USA, 2021; pp. 435–438.